(S.M. and K.N.) who were blinded to the treatment assignments performed the morphological analyses.

Thromboelastogram assays

Whole blood hemostatic parameters before, and at 30 and 180 min after vascular narrowing were measured using a ROTEM analyzer (Pentapharm GmbH, Munich, Germany). Blood samples were collected from the central ear artery into 3.8% sodium citrate (9:1, v/v), and 300-μL portions were transferred into the ROTEM reaction chamber. The blood was incubated with a monoclonal anti-TF antibody (10 μg mL^{-1}; American Diagnostica Inc., Greenwich, CT, USA) or with control mouse IgG (10 μg mL^{-1}; Chemicon International Inc., California, USA) and then re-calcified with 20 μL of 200 mmol L^{-1} $CaCl_2$ before clot formation was measured in duplicate using the standard NATEG evaluation parameters provided by the manufacturer. Rabbit plasma clotting time induced by rabbit brain thromboplastin (Thromboplastin C plus; Sysmex, Kobe, Japan) at a 1:4 dilution was significantly prolonged by the anti-TF antibody, compared with control IgG (control IgG; 114, 88–133 s vs. anti-rabbit TF antibody; 230, 144–301 s, $P < 0.05$, $n = 4$). We determined the following parameters: clotting time (CT), namely the duration between recalcification and the start of clot formation; maximal clot firmness (MCF) (mm), MCF-t; time at MCF, and lysis onset time (LOT), that is, time at 75% MCF. These parameters describe the following phases of the clotting process: initiation (CT), termination/final clot strength (MCF), velocity of clot formation (MCF-t) and fibrinolysis (LOT) [16].

Scanning electron microscopy

The femoral arteries (5 mm of post-stenotic region) were dissected out, opened longitudinally and further immersion-fixed in 4% neutralized formaldehyde and 1% glutaraldehyde in 0.1 mol L^{-1} phosphate buffer for 12 h at 4 °C. The femoral arteries were post-fixed with 2% OsO_4 in phosphate buffer for 90 min at room temperature, dehydrated in a graded series of t-butyl alcohol, freeze dried and sputter-coated with platinum and palladium. The post-stenotic region was examined with an S-4800 scanning electron microscope (SEM; Hitachi, Hitachi, Japan).

Number of apoptotic cells in intima/neointima after vascular narrowing

The numbers of apoptotic cells in the intima and neointima before and after vascular narrowing was assessed by terminal deoxynucleotidyl transferase-mediated deoxyuridine triphosphate nick end labeling (TUNEL) assays. Paraffin sections (3 μm-thick) were stained with the MEBSTAIN Apoptosis Kit II (Medical and Biological Laboratories Co. Ltd., Nagoya, Japan), and the number of positive nuclei per vessel was measured by fluorescence microscopy (IX71; OLYMPUS, Tokyo, Japan). The sections were double-stained with the MEBSTAIN Apoptosis Kit II and anti-VWF (The Binding Site) or anti-muscle actin (HHF35, DAKO), and then visualized using a digital CCD camera (DP70, OLYMPUS). The number of TUNEL-positive nuclei is expressed as the ratio (%) of total nuclei in the intima and neointima.

Modeling of shear stress at the post-stenotic region

Computational fluid dynamics were simulated using a two-dimensional Navier-Stokes flow solver and thermo-fluid analysis software (FINAS/CFD; ITOCHU Techno-Solutions Corporation, Tokyo, Japan). Blood rheology was assumed to be Newtonian and vessel boundaries were considered stationary and rigid. The model was based on the geometry shown in Fig. 4A with typical values for blood density and viscosity [17]. Flow volume was defined as 6 mL min^{-1} based on measurements *in vivo* with a transit time blood flow meter (T106; Transonic Systems Inc., Ithaca, NY, USA).

Statistical analysis

Results are expressed as medians and interquartile ranges, or as individual dots. Differences for individual groups were statistically evaluated using the Mann–Whitney *U*-test, Kruskal–Wallis test with Dunn's multiple comparison test, Wilcoxon's signed rank test, two-way repeated measures ANOVA or Fisher's exact test (GraphPad Prizm 4.03; GraphPad Software Inc., San Diego, CA, USA). $P < 0.05$ was considered statistically significant.

Results

Development of SMC-rich neointima with TF expression at 3 weeks after balloon injury

Neointima composed of SMCs and extracellular matrix with a few macrophages developed at 3 weeks after balloon injury to the left femoral artery. The luminal surface was completely lined by endothelial cells (Supplemental Fig. S1). Rabbit plasma clotting time was shorter in SMC-rich neointima with media (median, 391; range, 304 – 542 s; $n = 5$) than in normal intima with media (> 1000 s, $n = 5$, $P < 0.01$) and inhibited by rTFPI (> 1000 s, $n = 5$, $P < 0.01$). These results indicate that SMC-rich neointima had high levels of TF-dependent thrombogenic activity.

Disrupted blood flow after vascular narrowing

Figure 1A,B shows color Doppler images before and after vascular narrowing of the femoral arteries with SMC-rich neointima. The blood flow image at the post-stenotic region comprised a mosaic of mixed anterograde and retrograde blood flow (Fig. 1B). We measured blue and yellow areas during systole to evaluate the mosaic using a color imaging morphometry system. The colored areas were increased 5-fold after vascular narrowing (Fig. 1C), confirming that blood flow was indeed disturbed at the post-stenotic region. The mean

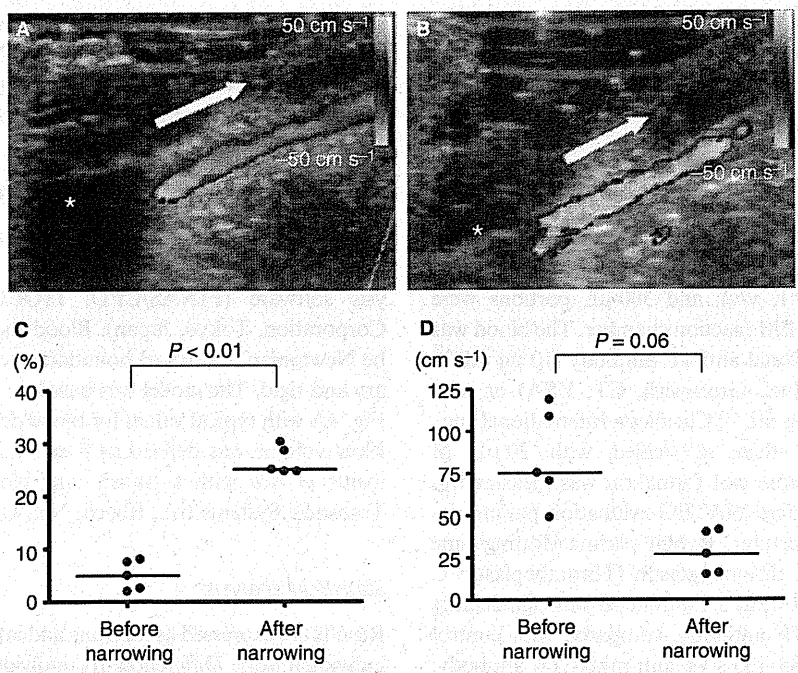

Fig. 1. Color Doppler images, mosaic area and flow velocity before and after vascular narrowing of femoral artery with smooth muscle cell (SMC)-rich neointima. Representative color Doppler images before (A) and after (B) narrowing of femoral artery. Arrows and asterisks indicate flow direction and acoustic shadow by vascular occluder, respectively. (C) Color Doppler mosaic area before and after vascular narrowing. (D) Blood flow velocity before and after vascular narrowing at the 2-mm post-stenosis region.

flow velocity at the region at 2 mm post-stenosis was decreased after vascular narrowing, but the difference was not statistically significant (Fig. 1D).

Erosive injury and thrombus formation on SMC-rich neointima after vascular narrowing

Figure 2A and Supplemental Fig. S2 show light microscopic features of the longitudinal section of the neointima at the post-stenotic region 15 min after vascular narrowing. The neointimal cells at this region were broadly detached, and associated with platelet adhesion to the sub-endothelium. SEM and immunohistochemistry also revealed broad desquamation of endothelial cells at the post-stenotic region and exposed subendothelial tissue covered with a monolayer or small aggregated platelets (Fig. 2B, Supplemental Fig. S3A,B). In addition, SMCs were frequently detached from the surface region of neointima in the endothelial desquamated areas (Fig. 2C, Supplemental Fig. S3C, D). These findings were similar to those of plaque erosion in human arteries. Mural thrombi developed after 30 min on the injured neointima (Fig. 2D), and then occlusive thrombi were generated in 3/5 vessels after 180 min (Fig. 2E, Table 1). Detached SMCs were involved in the thrombus (Supplemental Fig. S3E,F). To assess the degree of erosive injury, the length of endothelial detachment was measured at the post-stenotic region. The loss of endothelial covering was evident in normal and SMC-rich neointima 15 and 30 min after the vascular narrowing. The intimal injury significantly progressed 3 h after the vascular narrowing (Fig. 2F). The thrombi that developed on the neointima consisted of a mixture of aggregated platelets and a considerable amount of fibrin (Fig. 2G upper row). The same narrowing of normal femoral arteries also induced endothelial detachment and generated small mural platelet thrombi, but neither fibrin nor occlusive thrombi developed (Fig. 2G lower row, Table 1). Immunopositive areas for GP IIb/IIIa and/or fibrin in thrombi on the neointima were larger than those on the normal intima at 30 min after vascular narrowing (Fig. 2H).

Thromboelastogram assay

Whole blood hemostatic parameters before, and at 30 and 180 min after vascular narrowing did not significantly differ, and prior incubation with either anti-TF antibody or control IgG did not affect the parameters before and at 30 and 180 min after vascular narrowing (Table 2). This indicated that focal vascular narrowing does not affect systemic whole blood coagulability.

TUNEL-positive nuclei in intima/neointima after vascular narrowing

Figure 3 shows fluorescent TUNEL double-staining for VWF (Fig. 3A,C) or SMCs (Fig. 3B,D), and the number of TUNEL-positive nuclei in the intima and neointima (Fig. 3E). The intima and neointima were completely lined by endothelial cells in the absence of vascular narrowing (Fig. 3A). The TUNEL-positive nuclei were occasionally detectable after vascular

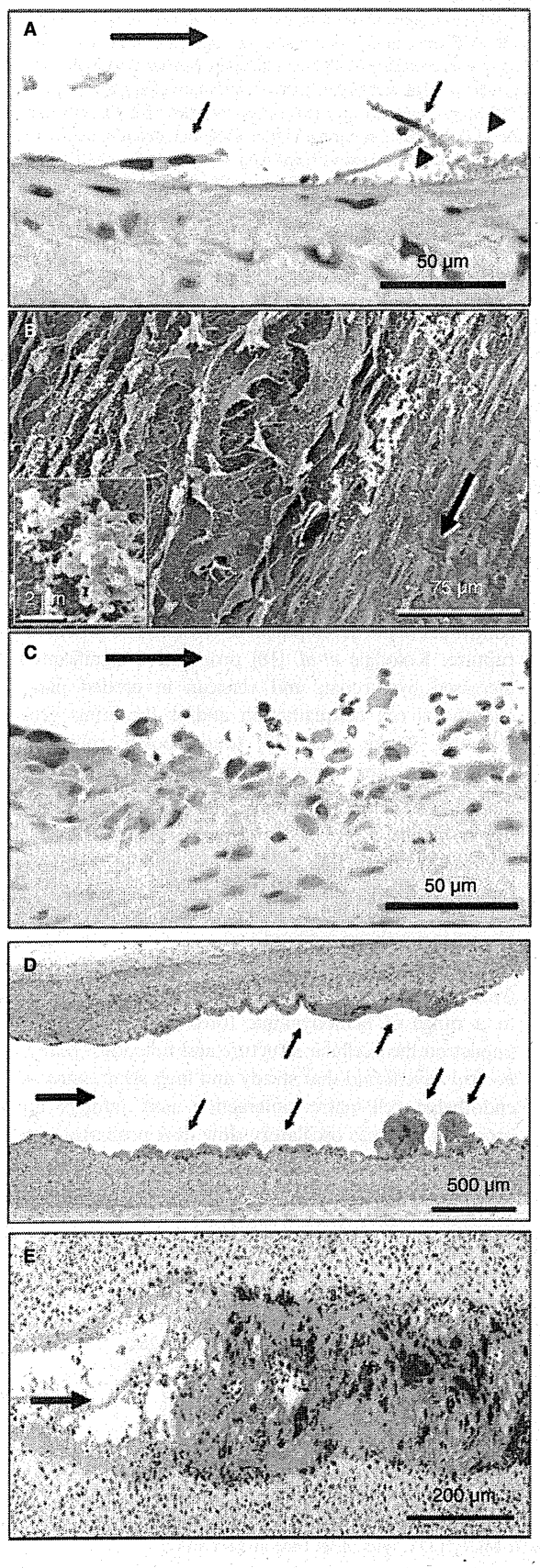

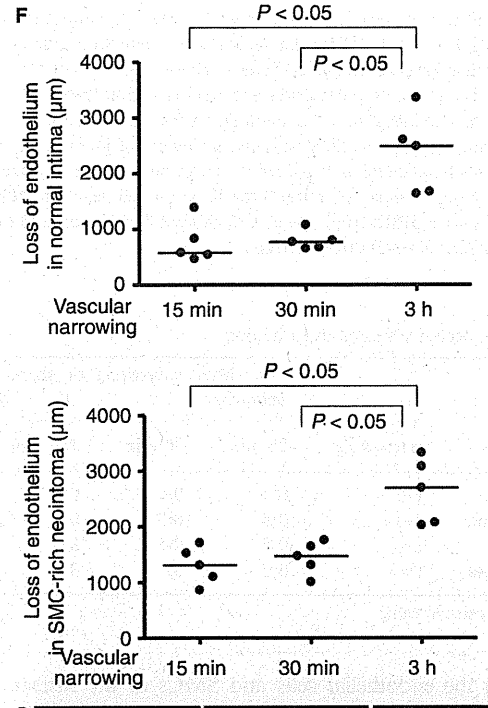

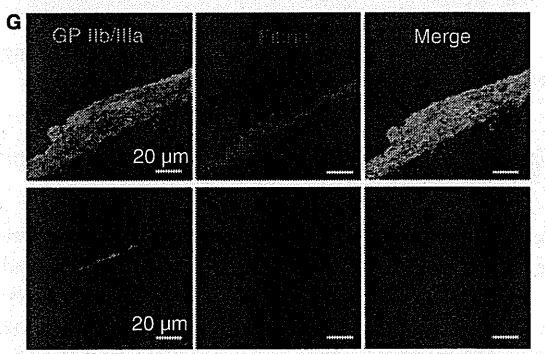

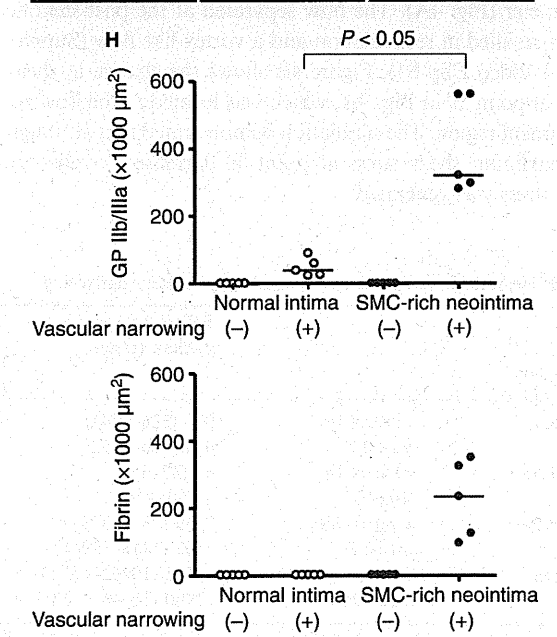

Fig. 2. Representative images of superficial erosive injury of smooth muscle cell (SMC)-rich neointima and thrombus formation at the post-stenotic region. A, C, D and E (HE stain), B (SEM). Large arrows indicate flow direction. (A, B, C) Erosive injury 15 min after vascular narrowing. Endothelial detachment (small arrows) accompanies platelet adhesion (arrow heads) at 1,000 μm from occluder (A). Sub-endothelium associated with platelet adhesion and aggregation is exposed on the left side, and residual endothelial cell layer is present on right side (inset, high magnification of aggregated platelets) (B). SMCs have detached at the surface of neointima at 1,500 μm from occluder (C). (D) Mural (small arrows) and (E) occlusive (asterisk) thrombi have formed at 30 and 180 min, respectively, after vascular narrowing. (F) Length of endothelial detachment in normal and in SMC-rich neointima after vascular narrowing at post-stenotic region measured by image analysis in longitudinal sections immunostained with anti-von Willebrand factor (VWF) antibody. (G) Immunofluorescent images of mural thrombi on injured neointima (upper row) and intima (lower row) 30 min after vascular narrowing. Fluorecein isothiocyanate-labeled GPIIb-IIIa is green, Cy3-labeled fibrin is red, and merged image is yellow. (H) Areas immunopositive for GPIIb-IIIa and fibrin in thrombi 30 min after femoral artery narrowing.

Table 1 Rate of occlusive thrombus formation

Femoral artery	Vascular narrowing	Time after narrowing or sham operation		
		15 min	30 min	180 min
Normal intima	(−)	0/5	0/5	0/5
SMC-rich intima	(−)	0/5	0/5	0/5
Normal intima	(+)	0/5	0/5	0/5
SMC-rich intima	(+)	0/5	0/5	3/5

SMC, smooth muscle cells.

narrowing in the endothelial cells and SMCs of the surface region of the neointima, whereas no nuclei were positive in the intima or the neointima in the absence of vascular narrowing (Fig. 3A–E).

Computational simulation of shear stress at the post-stenotic region

To assess changes in shear stress induced by vascular narrowing, we simulated the vessel structure of the rabbit artery and blood flow dynamics using thermo-fluid analysis software based on measurements taken *in vivo* using a transit time blood flow meter (Fig. 4A). The flow separated at the post-stenotic region resulted in recirculation and a vortex-like flow (Supplemental Video Clip S1). Figure 4B shows the change in shear stress at point 'a' in Fig. 4A, which was located at the flow reattachment region. The simulation demonstrated that although the maximum shear stress at point 'a' decreased, oscillatory shear stress was generated.

Discussion

The present study demonstrated that post-stenotic disturbed blood flow and oscillatory shear stress induced erosive damage and thrombus formation on SMC-rich neointima.

Although plaque rupture is the main cause of coronary thrombosis, plaque erosion is responsible for 20%–40% of acute thrombotic events. The interface of the eroded surface characteristically involves endothelial detachment and consists predominantly of SMCs and proteoglycans with minimal or absent inflammation [3,4,6]. The absence of significant inflammation suggests that this condition does not significantly contribute to the development of erosion, in contrast to plaque rupture. Kolodgie *et al.* [18] proposed a significant role of increased hyaluronan and versican in eroded plaques for endothelial cell desquamation and/or thrombus generation. Recently, Burke *et al.* [19] found polymorphisms among thrombospondins, a family of extracellular matrix proteins that regulate cell adhesion and migration [20] in sudden death due to plaque erosion, but not plaque rupture. These lines of evidence suggest that matrix changes in plaques would predispose them to erosion. However, the trigger of endothelial detachment and erosive injury of SMC-rich atherosclerotic plaque is poorly understood.

One modulator of plaque erosion might be blood flow dynamics. Vascular endothelial cells are continuously exposed to a range of hemodynamic forces that have considerable impact on their cellular structure and functions. Many studies *in vitro* have found that steady and high shear stress stabilizes endothelial cell–matrix interaction and inhibits apoptotic processes, whereas oscillatory slow flow promotes endothelial

Table 2 Hemostatic parameters before and after vascular narrowing

Parameters		Before narrowing median (range) $n = 5$	30 min after median (range) $n = 5$	180 min after median (range) $n = 5$	P
CT (sec)	control IgG	997 (686–1241)	1321 (927–1811)	991 (890–1260)	0.41
	anti-TF	904 (936–1152)	1118 (934–1703)	855 (429–1504)	
MCF (mm)	control IgG	61 (47–65)	56 (53–62)	61 (58–62)	0.85
	anti-TF	57 (49–65)	57 (53–64)	61 (54–66)	
MCF-t (sec)	control IgG	2549 (2343–3758)	3022 (1998–3946)	2980 (1961–3362)	0.18
	anti-TF	2503 (1418–3396)	2665 (2255–3755)	2246 (1941–2528)	
LOT (sec)	control IgG	13695 (10602–15721)	14353 (12067–15904)	13070 (10780–13233)	0.94
	anti-TF	12900 (10546–16338)	14492 (11229–15451)	13581 (10813–13688)	

CT, clotting time, < 2 mm; MCF, maximum clot firmness; MCF-t, time at MCF; LOT, lysis onset time at 75% MCF.

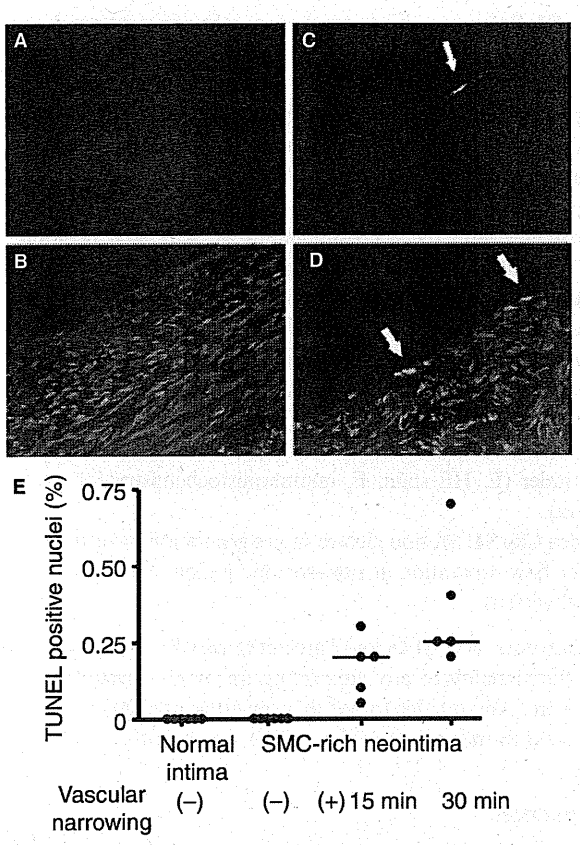

Fig. 3. Representative merged fluorescent images and numbers of TUNEL-positive nuclei. Fluorescent images of neointima in the absence of vascular narrowing (A, B) or at 15 min after vascular narrowing (C, D) stained with anti- von Willebrand factor (VWF) (A, C) or anti-muscle actin (B, D) antibody and TUNEL labeling. Arrows indicate TUNEL-positive endothelial cells (B) or smooth muscle cells (SMCs) (D). (E) Rate (%) of TUNEL-positive nuclei in intima and neointima before and after vascular narrowing.

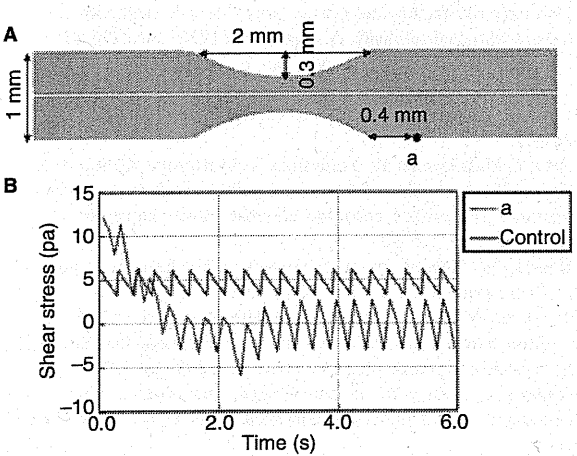

Fig. 4. Computational simulation of shear stress at the post-stenotic region. Schema of stenotic vessel model. Variation of shear stress at point (a) in Fig. 4A. Control indicates calculated shear stress in non-stenotic vessel model.

cell apoptosis [7,21]. A pathological study of human carotid atherosclerotic plaques has demonstrated that endothelial cells preferentially undergo apoptosis, the frequency of which is obviously increased at downstream parts of plaques where lower shear stress prevails relative to the upstream regions [8]. The number of TUNEL-positive endothelial cells was increased, more endothelial cells were denuded and more thrombus was formed in rabbit femoral arteries treated with apoptosis-inducing staurosporine [22]. These results indicate that endothelial apoptosis lead to endothelial denudation and thrombosis *in vivo*, and low shear stress is a powerful inducer of apoptosis. In addition to physical stress, low or turbulent shear stress can induce endothelial cells and SMCs to undergo apoptosis via apoptotic cell signaling and/or loss of survival signaling [23,24]. Moreover, Sho *et al.* [25] demonstrated that a sudden decrease in wall shear stress induces endothelial cell apoptosis in the rabbit carotid artery. Our results also showed that endothelial cells and SMCs undergo apoptosis at regions of post-stenotic low shear stress. However, the number of apoptotic cells was very low, and the damage involved not only endothelium but also SMCs and the surrounding extracellular matrix in the neointima. The histologic findings were very similar to those of plaque erosion found in human pathological studies [3,4,6]. Low shear stress up-regulates matrix metalloproteinases (MMPs), particularly MMP-2 and MMP-9 in vascular cells, resulting in focal degradation of extracellular matrix [26]. However, erosive injury was detected in the present study within 15 min of vascular narrowing. Fry [11] reported that acute aortic stenosis can produce turbulent shear stress on endothelial cells at the post-stenotic region, resulting in rhomboidal deformation of these cells and surface erosion. This evidence suggests that direct hemodynamic forces play a crucial role in lesion development. Computational simulation showed that vascular narrowing decreased the mean value of the shear stress at the flow reattachment region, but generated oscillatory shear stress. Although the computational simulation in the present study could not evaluate detailed changes in shear stress, the anterograde and retrograde oscillatory shear stress cycle might be a potent trigger for erosive injury of SMC-rich neointima.

The size and constituents of thrombi on eroded normal and eroded SMC-rich neointima differed and TF-dependent coagulation activity was obviously elevated in the neointima of this animal model as it is in human plaques [2,27]. Although a few studies have demonstrated that circulating TF plays a functional role in promoting thrombus growth *in vivo* [28,29], the functional role of circulating TF remains controversial [30,31]. Vascular narrowing or anti-rabbit TF antibody did not affect whole blood hemostatic parameters in the rabbits and no fibrin was generated in thrombi on eroded normal intima, thus indicating that TF was derived from eroded neointima rather than circulating TF playing a crucial role in fibrin and thrombus growth. Vascular narrowing led to progression of neointimal injury and thrombotic occlusion in 60% of arteries with neointima. Although we could not assess the exact mechanisms in the present study, disturbed blood flow drives

platelet aggregation and thrombus growth [32–34]. In addition, elevated distal vascular resistance due to microembolism together with microvascular constriction could promote these processes [35,36]. We previously showed that blood flow reduction induced by distal vasoconstriction facilitates thrombus propagation and also thrombotic occlusion in this animal model [15].

Several limitations are associated with this study. We examined only one degree of vascular narrowing because the investigated arteries were quite small. Therefore, which levels of stenosis or oscillatory shear stress lead to erosive injury could not be assessed. The ultrasonographic resolution of blood flow images was not high enough for comparison with computational fluid simulation. Computational simulation analysis was performed under steady-state wall motion and stiffness, and does not correspond to rheological conditions in individual vessels. Further studies are required to address these issues to further clarify the pathogenesis of plaque erosion.

In conclusion, disturbed blood flow induced superficial erosive injury and platelet-fibrin thrombus formation on SMC-rich neointima in rabbit femoral arteries, some of which resulted in vessel occlusion. These findings suggest that disturbed blood flow associated with vasoconstriction or atherosclerotic stenosis could induce plaque erosion and thrombosis.

Addendum

T. Sumi, A. Yamashita, T. Imamura, K. Kitamura, S. Tamura and Y. Asada contributed to the concept and design. T. Sumi, A. Yamashita, S. Matsuda, S. Goto, K. Nishihira, E. Furukoji, H. Sugimura, H. Kawahara and Y. Asada contributed to analysis and/or interpretation of data, and critical writing of the manuscript.

Acknowledgements

This study was supported in part by Grants-in-Aid for Scientific Research in Japan (Nos. 19790293, 20390102, 20591481) from the Ministry of Education, Science, Sports and Culture of Japan.

Disclosure of Conflicts of interests

The authors state that they have no conflict of interest.

Supporting Information

Additional Supporting Information may be found in the online version of this article:

Fig. S1. Representative light microphotograph of femoral artery 3 weeks after balloon injury. Neointima (N) comprises SMCs and extracellular matrix, and is completely lined by endothelial cells (arrows). M, media; Ad, adventitia (HE stain).

Fig. S2. Representative microphotographs of neointima distant from occluder at 15 min after vascular narrowing. Erosive injury of neointima is broadly present at the post-stenotic region (small arrows). Large arrows indicate flow direction. N, neointima; M, media; Ad, adventitia (HE stain).

Fig. S3. Representative light and immunomicrophotograph of superficial erosive injury of SMC-rich neointima and thrombus formation. Superficial erosive injury of SMC-rich neointima 15 min after vascular narrowing (A–D). Detachment of endothelial cells (arrows) at 1000 μm from occluder (A, HE stain; B, immunohistochemistry for VWF). Detachment of SMCs (arrows) at 1500 μm from occluder (C, HE stain; D, immunohistochemistry for muscle actin). Erosive injury and thrombus formation 3 h after vascular constriction (E, F). Involvement of SMCs in thrombus (arrows) at 2500 μm from occluder (E, HE stain; F, immunohistochemistry for muscle actin).

Video Clip S1. Motion picture shows generation of vertical flow after flow separation at post-stenotic region. Vectors indicate flow velocity.

Please note: Wiley-Blackwell are not responsible for the content or functionality of any supporting materials supplied by the authors. Any queries (other than missing material) should be directed to the corresponding author for the article.

References

1 Virmani R, Kolodgie FD, Burke AP, Farb A, Schwartz SM. Lessons from sudden coronary death: a comprehensive morphological classification scheme for atherosclerotic lesions. *Arterioscler Thromb Vasc Biol* 2000; **20**: 1262–75.

2 Fuster V, Moreno PR, Fayad ZA, Corti R, Badimon JJ. Atherothrombosis and high-risk plaque: part I: evolving concepts. *J Am Coll Cardiol* 2005; **46**: 937–54.

3 Farb A, Burke AP, Tang AL, Liang TY, Mannan P, Smialek J, Virmani R. Coronary plaque erosion without rupture into a lipid core: a frequent cause of coronary thrombosis in sudden coronary death. *Circulation* 1996; **93**: 1354–63.

4 Burke AP, Farb A, Malcom GT, Liang YH, Smialek J, Virmani R. Coronary risk factors and plaque morphology in men with coronary disease who died suddenly. *N Engl J Med* 1997; **336**: 1276–82.

5 Arbustini E, Dal Bello B, Morbini P, Burke AP, Bocciarelli M, Specchia G, Virmani R. Plaque erosion is a major substrate for coronary thrombosis in acute myocardial infarction. *Heart* 1999; **82**: 269–72.

6 Sato Y, Hatakeyama K, Yamashita A, Marutsuka K, Sumiyoshi A, Asada Y. Proportion of fibrin and platelets differs in thrombi on ruptured and eroded coronary atherosclerotic plaques in humans. *Heart* 2005; **91**: 526–30.

7 Malek AM, Alper SL, Izumo S. Hemodynamic shear stress and its role in atherosclerosis. *JAMA* 1999; **282**: 2035–42.

8 Tricot O, Mallat Z, Heymes C, Belmin J, Lesèche G, Tedgui A. Relation between endothelial cell apoptosis and blood flow direction in human atherosclerotic plaques. *Circulation* 2000; **101**: 2450–3.

9 Chien S, Li S, Shyy YJ. Effects of mechanical forces on signal transduction and gene expression in endothelial cells. *Hypertension* 1998; **31**: 162–9.

10 Topper JN, Gimbrone MA Jr. Blood flow and vascular gene expression: fluid shear stress as a modulator of endothelial phenotype. *Mol Med Today* 1999; **5**: 40–6.

11 Fry DL. Acute vascular endothelial changes associated with increased blood velocity gradients. *Circ Res* 1968; **22**: 165–97.
12 Joris I, Zand T, Majno G. Hydrodynamic injury of the endothelium in acute aortic stenosis. *Am J Pathol* 1982; **106**: 394–408.
13 Oshima S, Yasue H, Ogawa H, Okumura K, Matsuyama K. Fibrinopeptide A is released into the coronary circulation after coronary spasm. *Circulation* 1990; **82**: 2222–5.
14 Miyamoto S, Ogawa H, Soejima H, Takazoe K, Kajiwara I, Shimomura H, Sakamoto T, Yoshimura M, Kugiyama K, Yasue H, Ozaki Y. Enhanced platelet aggregation in the coronary circulation after coronary spasm. *Thromb Res* 2001; **103**: 377–86.
15 Yamashita A, Furukoji E, Marutsuka K, Hatakeyama K, Yamamoto H, Tamura S, Ikeda Y, Sumiyoshi A, Asada Y. Increased vascular wall thrombogenicity combined with reduced blood flow promotes occlusive thrombus formation in rabbit femoral artery. *Arterioscler Thromb Vasc Biol* 2004; **24**: 2420–4.
16 Yamashita A, Matsuda S, Moriguchi-Goto S, Takahashi M, Sugita Ç, Sumi T, Imamura T, Kitamura K, Asada Y. Thrombin generation by intimal tissue factor contributes to thrombus formation on macrophage-rich neointima but not normal intima of hyperlipidemic rabbits. *Atherosclerosis* 2009; **206**: 418–26.
17 Fung YC. Biomechanics: mechanical properties of living tissues, 2nd edn. New York: Springer-Verlag, 1993.
18 Kolodgie FD, Burke AP, Farb A, Weber DK, Kutys R, Wight TN, Virmani R. Differential accumulation of proteoglycans and hyaluronan in culprit lesions: insights into plaque erosion. *Arterioscler Thromb Vasc Biol* 2002; **22**: 1642–8.
19 Burke A, Creighton W, Tavora F, Li L, Fowler D. Decreased frequency of the 3'UTR T>G single nucleotide polymorphism of thrombospondin-2 gene in sudden death due to plaque erosion. *Cardiovasc Pathol* in press.
20 Adams JC, Lawler J. The thrombospondins. *Int J Biochem Cell Biol* 2004; **36**: 961–8.
21 Mallat Z, Tedgui A. Current perspective on the role of apoptosis in atherothrombotic disease. *Circ Res* 2001; **88**: 998–1003.
22 Durand E, Scoazec A, Lafont A, Boddaert J, Al Hajzen A, Addad F, Mirshahi M, Desnos M, Tedgui A, Mallat Z. In vivo induction of endothelial apoptosis leads to vessel thrombosis and endothelial denudation: a clue to the understanding of the mechanisms of thrombotic plaque erosion. *Circulation* 2004; **109**: 2503–6.
23 Davies PF, Remuzzi A, Gordon EJ, Dewey CF Jr, Gimbrone MA Jr. Turbulent fluid shear stress induces vascular endothelial cell turnover in vitro. *Proc Natl Acad Sci USA* 1986; **83**: 2114–7.
24 Apenberg S, Freyberg MA, Friedl P. Shear stress induces apoptosis in vascular smooth muscle cells via an autocrine Fas/FasL pathway. *Biochem Biophys Res Commun* 2003; **310**: 355–9.
25 Sho E, Sho M, Singh TM, Xu C, Zarins CK, Masuda H. Blood flow decrease induces apoptosis of endothelial cells in previously dilated arteries resulting from chronic high blood flow. *Arterioscler Thromb Vasc Biol* 2001; **21**: 1139–45.
26 Chatzizisis YS, Coskun AU, Jonas M, Edelman ER, Feldman CL, Stone PH. Role of endothelial shear stress in the natural history of coronary atherosclerosis and vascular remodeling: molecular, cellular, and vascular behavior. *J Am Coll Cardiol* 2007; **49**: 2379–93.
27 Hatakeyama K, Asada Y, Marutsuka K, Sato Y, Kamikubo Y, Sumiyoshi A. Localization and activity of tissue factor in human aortic atherosclerotic lesions. *Atherosclerosis*. 1997; **133**: 213–9.
28 Himber J, Wohlgensinger C, Roux S, Damico LA, Fallon JT, Kirchhofer D, Nemerson Y, Riederer MA. Inhibition of tissue factor limits the growth of venous thrombus in the rabbit. *J Thromb Haemost* 2003; **1**: 889–95.
29 Chou J, Mackman N, Merrill-Skoloff G, Pedersen B, Furie BC, Furie B. Hematopoietic cell-derived microparticle tissue factor contributes to fibrin formation during thrombus propagation. *Blood* 2004; **104**: 3190–7.
30 Day SM, Reeve JL, Pedersen B, Farris DM, Myers DD, Im M, Wakefield TW, Mackman N, Fay WP. Macrovascular thrombosis is driven by tissue factor derived primarily from the blood vessel wall. *Blood* 2005; **105**: 192–8.
31 Butenas S, Orfeo T, Mann KG. Tissue factor activity and function in blood coagulation. *Thromb Res* 2008; **122**(Suppl 1): S42–6.
32 Wootton DM, Markou CP, Hanson SR, Ku DN. A mechanistic model of acute platelet accumulation in thrombogenic stenoses. *Ann Biomed Eng* 2001; **29**: 321–9.
33 Hathcock JJ. Flow effects on coagulation and thrombosis. *Arterioscler Thromb Vasc Biol* 2006; **26**: 1729–37.
34 Nesbitt WS, Westein E, Tovar-Lopez FJ, Tolouei E, Mitchell A, Fu J, Carberry J, Fouras A, Jackson SP. A shear gradient-dependent platelet aggregation mechanism drives thrombus formation. *Nat Med* 2009; **15**: 665–73.
35 Topol EJ, Yadav JS. Recognition of the importance of embolization in atherosclerotic vascular disease. *Circulation* 2000; **101**: 570–80.
36 Skyschally A, Erbel R, Heusch G. Coronary microembolization. *Circ J* 2003; **67**: 279–86.

Peptides 31 (2010) 889–892

Contents lists available at ScienceDirect

Peptides

journal homepage: www.elsevier.com/locate/peptides

Plasma and tissue levels of proangiotensin-12 and components of the renin–angiotensin system (RAS) following low- or high-salt feeding in rats

Sayaka Nagata[a,*], Johji Kato[b], Kenji Kuwasako[b], Kazuo Kitamura[a]

[a] Circulatory and Body Fluid Regulation, Faculty of Medicine, University of Miyazaki, 5200 Kihara, Kiyotake, Miyazaki 889-1692, Japan
[b] Frontier Science Research Center, University of Miyazaki, Kiyotake, Miyazaki 889-1692, Japan

ARTICLE INFO

Article history:
Received 16 July 2009
Received in revised form 10 February 2010
Accepted 10 February 2010
Available online 19 February 2010

Keywords:
Proangiotensin-12
Renin–angiotensin system
Dietary salt

ABSTRACT

The renin–angiotensin system (RAS) is an essential regulator of the blood pressure and body fluid balance, but the processing cascade or role of the tissue RAS remains obscure. Proangiotensin-12 (proang-12), a novel angiotensin peptide recently discovered in rat tissues, is assumed to function as a factor of the tissue RAS. To investigate the tissue production of proang-12, we measured the circulating and tissue components of the RAS including proang-12 following low-, normal-, or high-salt feeding in rats. Twelve-week-old male Wistar rats were fed a low-salt 0.3% NaCl or high-salt 8% NaCl diet for 7 days and compared with those fed a normal-salt diet of 0.7% NaCl. Low-salt feeding elevated the plasma renin activity and aldosterone concentration, resulting in significant increases in Ang I and Ang II levels in the plasma or kidney tissue, as compared with the normal- or high-salt group. Despite the increases in plasma renin activity, Ang I, and Ang II, the proang-12 levels in plasma and various tissues including the kidneys, small intestine, cardiac ventricles, and brain remained unchanged following low-salt feeding. These results suggest that peptide levels of proang-12 in rat plasma and tissues are regulated in a manner independent of the circulating RAS.

1. Introduction

The renin–angiotensin system (RAS) plays an important role in regulating the blood pressure and fluid balance. The protease enzyme renin cleaves angiotensinogen circulating in the blood to produce angiotensin I (Ang I), which, in the presence of angiotensin-converting enzyme (ACE), is converted to Ang II, a potent pressor peptide mediating the major actions of the RAS as a circulating hormone [4,18]. A number of studies have been conducted on the tissue RAS, the function of which is assumed to be regulated independently of the circulating RAS [1,7,16,19]. There are, however, many unanswered questions regarding the tissue RAS, such as the processing cascade of angiotensin peptides or roles in regulating the blood pressure or fluid balance. Proangiotensin-12 (proang-12) is a C-terminal extended form of Ang I (Ang I-Leu-Tyr) recently isolated and identified in the rat small intestine [17]. When injected intravenously into rats, proang-12 exerts vasoconstrictor and pressor effects, which are abolished by an ACE inhibitor or an Ang II type I receptor blocker, suggesting the role of this novel peptide as a precursor of Ang II. As the levels of proang-12 in various tissues including the heart, kidneys, and small intestine are much higher than in the blood, proang-12 is assumed to be a factor of the tissue RAS in rats [10,17,22]. However, there are also a number of unresolved issues concerning the production cascade and function of this novel peptide. In the present study, we measured the plasma and tissue levels of proang-12, Ang I, and Ang II in rats under the condition of low-salt feeding, where the systemic RAS is activated, in an effort to answer these important questions.

2. Materials and methods

2.1. Animals and experimental protocol

Male Wistar rats at 10 weeks of age were purchased from CHARLES RIVER LABORATORIES (Kanagawa, Japan) and maintained under a 12-h light/12-h dark cycle in specific pathogen-free conditions with a normal diet containing 0.7% NaCl for 14 days. Thereafter, the rats were randomly divided into three groups fed a low-, normal-, or high-salt diet containing NaCl of 0.3, 0.7, and 8% (ORIENTAL YEAST Co., Ltd., Tokyo, Japan), respectively ($n = 7$–8 in each group). Blood pressure levels were measured before and after the low- or high-salt feeding by means of the tail-cuff method (model BP-98A; Softron Co., Ltd., Tokyo, Japan). After the 7 days of feeding, blood samples were collected following decapitation into a tube containing 10 mg/ml EDTA and 500 KIU/ml aprotinin and immediately centrifuged at 3000 × *g* for 10 min at 4 °C to obtain the plasma.

* Corresponding author. Tel.: +81 985 85 9718; fax: +81 985 85 9718.
E-mail address: saya223@fc.miyazaki-u.ac.jp (S. Nagata).

0196-9781/$ – see front matter © 2010 Elsevier Inc. All rights reserved.
doi:10.1016/j.peptides.2010.02.008

The present study was performed in accordance with the Animal Welfare Act and with the approval of the University of Miyazaki Institutional Animal Care and Use Committee (2008-501-2).

2.2. Sample preparation for radioimmunoassay (RIA)

Tissues were carefully resected after decapitation and boiled for 10 min in 10 volumes of distilled H_2O. After boiling, acetic acid was added to the samples to a final concentration of 1.0 mol/l, as previously described [11,15]. The samples were then homogenized using a Polytron mixer and immediately centrifuged at 12 000 rpm for 20 min at 4 °C. Both the plasma and the tissue samples were applied to a Sep-Pak C18 cartridge and eluted with 60% acetonitrile in 0.1% trifluoroacetic acid. Eluted samples were lyophilized and store at −20 °C until RIA.

2.3. Measurement of proang-12 and other components of the RAS

To specifically detect proang-12 in tissues and plasma, we developed a RIA, as previously described, with antiserum raised against the C-terminal portion of the peptide [17]. The Ang I and Ang II levels in tissues and plasma were similarly determined using RIAs with the anti-C-terminal of Ang I and Ang II antisera purchased from Miles and CORTEX BIOCHEM, INC. (San Leandro, USA), respectively [8,13]. The angiotensinogen levels in plasma were determined by employing an ELISA purchased from Immuno-Biological Laboratories Co., Ltd. (Gunma, Japan). Plasma renin activity and aldosterone levels were measured using RIAs, as previously described [12].

2.4. Statistical analysis

Comparisons of all data were made employing analysis of variance (ANOVA) followed by Scheffe's tests. Values are presented as means ± SE, and significance was set at $P < 0.05$.

3. Results

No significant differences were noted in systolic and diastolic blood pressures (SBP and DBP, respectively) between the low-, normal-, or high-salt groups (SBP, 121 ± 5, 135 ± 3, 129 ± 4; DBP, 94 ± 3, 101 ± 3, 96 ± 4 mmHg). Fig. 1 shows the plasma renin activity as well as plasma aldosterone and angiotensinogen concentrations in the three groups of rats. Compared with the normal-salt group, a 117% increase was observed in the plasma renin activity in the low-salt group, and, accordingly, the plasma aldosterone concentration was increased by 120% (Fig. 1A and B). In contrast, both the plasma renin activity and the aldosterone concentration were reduced in the high-salt group, though the reductions were non-significant. The angiotensinogen level of plasma was slightly elevated by low-salt feeding, but the difference was non-significant (Fig. 1C).

Fig. 2 shows the plasma levels of proang-12, Ang I, and Ang II in the three groups. When compared with the normal-salt group, low-salt feeding resulted in a slight increase of plasma Ang I levels, and the Ang II level was elevated by 989% (Fig. 2B and C). Despite the increases in Ang I and Ang II, there was no significant difference in the plasma levels of proang-12 among the three groups. Similar changes were observed in tissue proang-12 levels in the kidneys (Fig. 3). In comparison with the normal-salt group, the Ang I and Ang II levels in the low-salt group were elevated by 85 and 57%, respectively; however, the proang-12 level remained unchanged. As shown in Fig. 4, we measured proang-12 levels in various tissues, but the differences were non-significant between the three groups except for those of the liver.

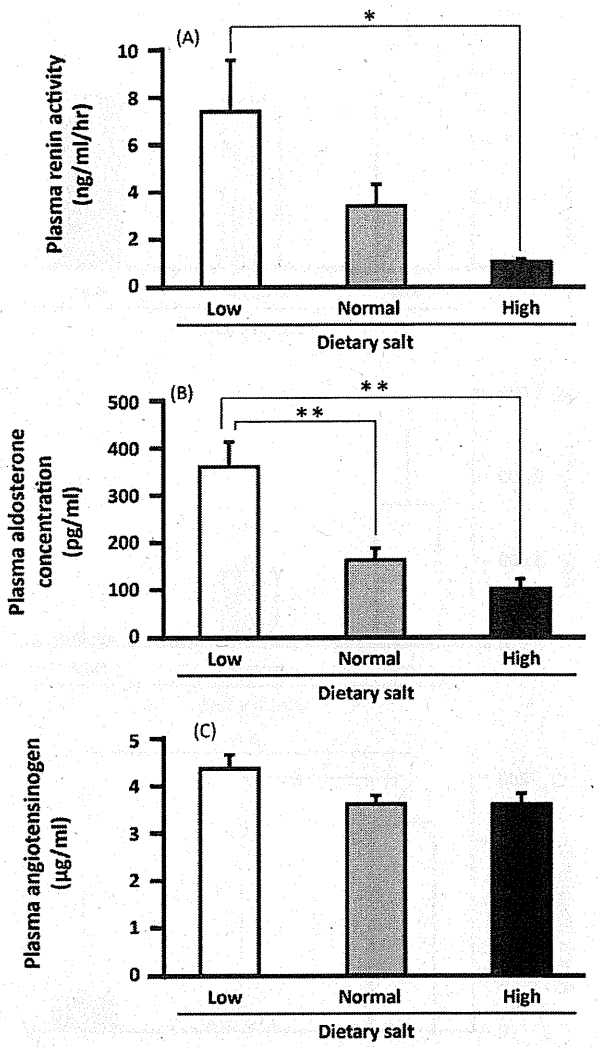

Fig. 1. Plasma renin activity (A), aldosterone (B), and angiotensinogen (C) levels in rats fed a low-, normal-, or high-salt diet. The results are shown as the means ± SE. $^{*}P < 0.05$, $^{**}P < 0.01$.

4. Discussion

Proang-12, a novel angiotensin peptide first identified in the rat small intestine, is thought to be produced from angiotensinogen and converted into Ang I or Ang II [17,21]. In the present study, we measured the plasma and tissue levels of proang-12 following low-salt feeding, which activated the systemic RAS, as evidenced by augmentations of plasma renin activity, aldosterone, and Ang I and II concentrations. In contrast to Ang I or Ang II in the plasma or tissues, the levels of proang-12 remained unchanged in rats fed the low-salt diet. On comparison of the plasma and tissue levels of peptides, proang-12 levels in various rat tissues were much higher than in plasma, suggesting a role for this peptide as a component of the tissue RAS. However, almost the opposite was the case for Ang I, and this was further evident in the plasma and kidneys of rats placed under low-salt conditions in the present study.

An important question is whether or not proang-12 is produced and processed by the action of renin in the systemic circulation or local tissues. To investigate the role of systemic renin, we previously measured tissue proang-12 levels following bilateral nephrectomy in rats. In that experiment, despite a marked reduction in the plasma levels of Ang I and Ang II, the tissue levels of

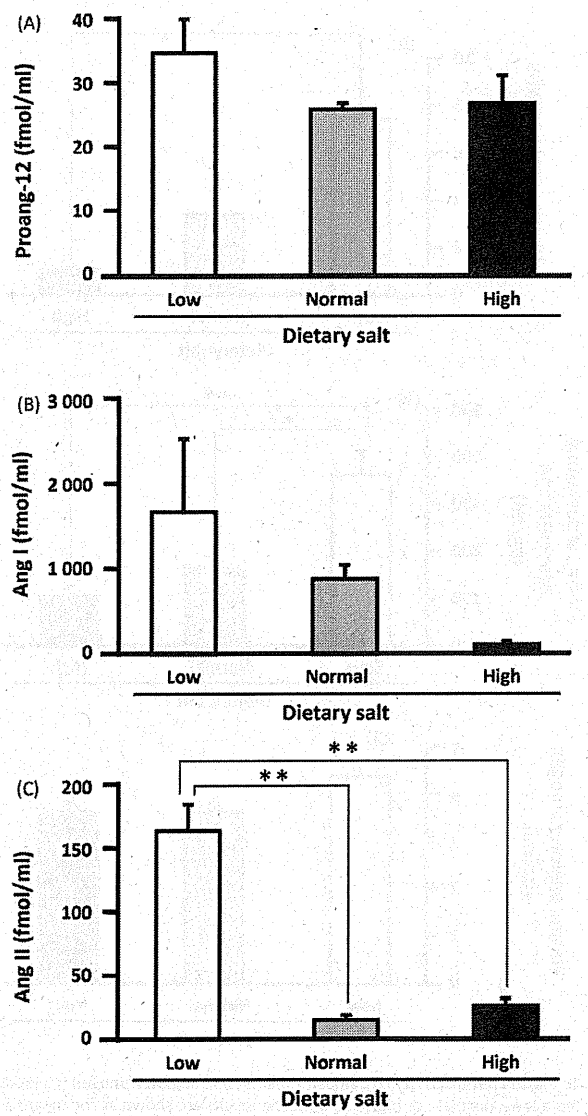

Fig. 2. Immunoreactive proangiotensin-12 (A), Ang I (B), and Ang II (C) levels in the plasma of rats fed a low-, normal-, or high-salt diet. The results are shown as the means ± SE. Proang-12 levels in the low-, normal-, and high-salt groups were 34 ± 5, 25 ± 1, and 26 ± 4 fmol/ml, respectively. $^{**}P<0.01$.

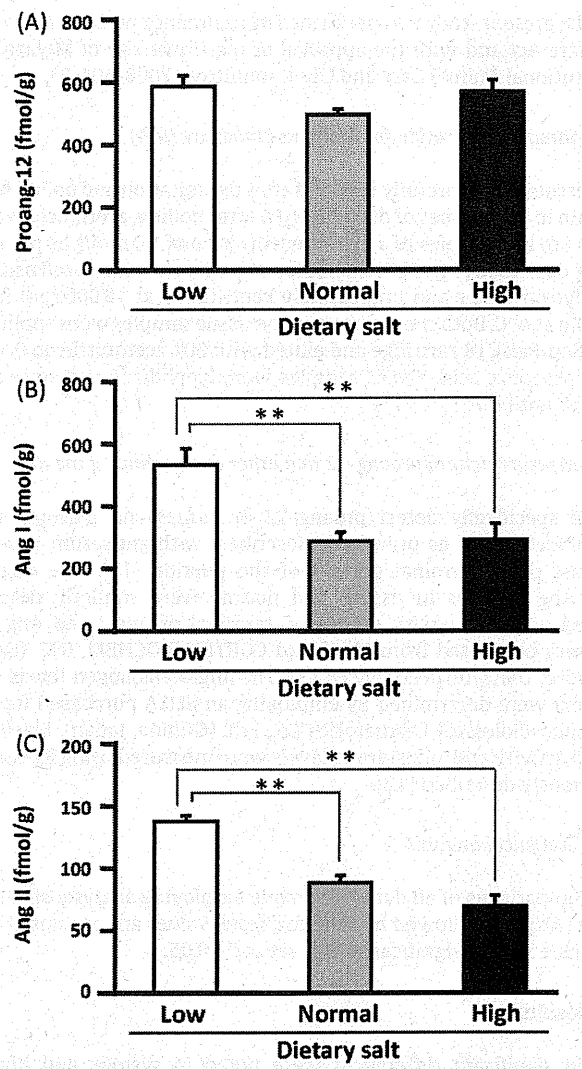

Fig. 3. Immunoreactive proangiotensin-12 (A), Ang I (B), and Ang II (C) levels in the kidney tissues of rats fed a low-, normal-, or high-salt diet. The results are shown as the means ± SE. $^{**}P<0.01$.

three angiotensin peptides were found to be elevated in the cardiac ventricles [6]. In the conversion of proang-12 to Ang I or other angiotensin peptides, a renin inhibitor failed to inhibit Ang I production from proang-12 in perfused rat hearts *ex vivo* [21]. Prosser et al. reported that chymase inhibition resulted in the attenuation of proang-12-induced cardiac damage following ischemia-perfusion in rat hearts *ex vivo*, suggesting that chymase is involved in the conversion of proang-12 to Ang I or Ang II [20]. In the present study, despite the increase in plasma renin activity induced by low-salt feeding, the tissue levels of proang-12 remained unchanged in a number of organs including the kidneys, heart, and small intestine. Collectively, it is unlikely that renin is involved in the production or processing of proang-12 in rats, and proang-12 levels in the plasma and tissues appear to be regulated independently of the systemic RAS.

There is a substantial amount of evidence suggesting the active roles of the local RAS in tissues including the kidneys, cardiac ventricles, and brain [2,3,5,17]. In the present study, both the Ang I and the Ang II levels in the kidney were elevated by low-salt feeding, a

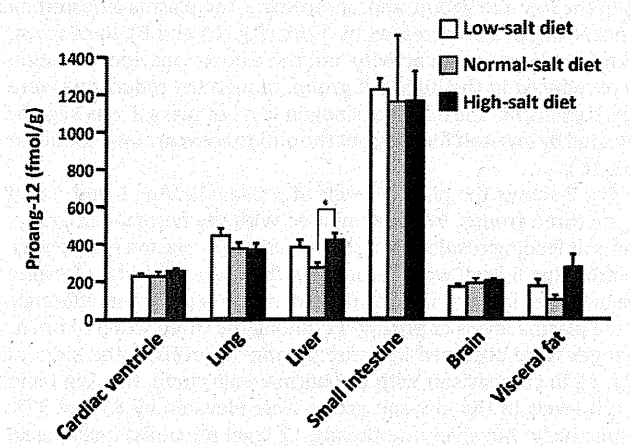

Fig. 4. Immunoreactive proangiotensin-12 levels in various tissues of rats fed a low-, normal-, or high-salt diet. The results are shown as the means ± SE. $^{*}P<0.05$.

finding consistent with the view that angiotensins intrarenally produced by renin play an active role in retaining sodium in the renal tubules [14]. Despite the augmentations of Ang I and Ang II in kidneys, we observed no increase in these peptide levels in the cardiac ventricles following low-salt feeding (data not shown). The brain is also an organ where the tissue RAS is assumed to play an active role because components of the RAS are expressed at a significant level [7,17]. Recently, Isa et al. reported that the neutralization of brain proang-12 by a specific antibody resulted in blood pressure reduction in mRen2 transgenic rats, suggesting a role of proang-12 in centrally modulating blood pressure in the rat brain [9]. In the present study, the blood pressure remained unchanged, and we observed no significant changes in tissue proang-12 levels of the kidneys, cardiac ventricles, or brain in the three groups of rats. However, those findings do not necessarily exclude the possibility that proang-12 participates in the regulation of electrolytes and water balance under low-salt conditions. An example is provided by the plasma angiotensinogen level as shown in Fig. 1, where no clear differences were noted between the three groups. Further studies need to be aimed to further specify the roles of this novel peptide in disorders of blood pressure or fluid balance, in which the tissue RAS is involved.

In summary, the proang-12 levels in tissues and plasma remained unchanged following low-salt feeding despite the activation of the systemic RAS in rats. The present findings support the notion that proang-12 is produced independently of renin in the systemic circulation, suggesting that the proang-12 levels in tissues and plasma are differentially modulated in rats.

Acknowledgment

The present study was partly supported by Grants-in-aid for Scientific Research from the Japan Society for the Promotion of Science.

References

[1] Campbell DJ. Circulating and tissue angiotensin systems. J Clin Invest 1987;79:1–6.
[2] Campbell DJ, Habener JF. Angiotensinogen gene is expressed and differentially regulated in multiple tissues of the rat. J Clin Invest 1986;78:31–9.
[3] Dzau VJ. Significance of the vascular renin–angiotensin pathway. Hypertension 1986;8:553–9.
[4] Dzau VJ, Burt DW, Pratt RE. Molecular biology of the renin–angiotensin system. Am J Physiol 1988;255:F563–73.
[5] Dzau VJ, Ingelfinger JR, Pratt RE. Regulation of tissue renin and angiotensin gene expressions. J Cardiovasc Pharmacol 1986;8(Suppl. 10):S11–6.
[6] Ferrario CM, Varagic J, Habibi J, Nagata S, Kato J, Chappell MC, et al. Differential regulation of angiotensin-(1-12) in plasma and cardiac tissue in response to bilateral nephectomy. Am J Physiol Heart Circ Physiol 2009;296: H1184–92.
[7] Fischer-Ferraro C, Nahmod VE, Goldstein DJ, Finkielman S. Angiotensin and renin in rat and dog brain. J Exp Med 1971;133:353–61.
[8] Ichiki Y, Kitamura K, Kangawa K, Kawamoto M, Matsuo H, Eto T. Distribution and characterization of immunoreactive adrenomedullin in human tissue and plasma. FEBS Lett 1994;338:6–10.
[9] Isa K, Garcia-Espinosa MA, Arnold AC, Pirro NT, Tommasi EN, Ganten D, et al. Chronic immunoneutralization of brain angiotensin-(1-12) lowers blood pressure in transgenic (mRen2) 27 hypertensive rats. Am J Physiol Regul Integr Comp Physiol 2009;297:R111–5.
[10] Jessup JA, Trask AJ, Chappell MC, Nagata S, Kato, Kitamura K, et al. Localization of the novel angiotensin peptide, angiotensin-12 [Ang-(1-12)], in heart and kidney of hypertensive and normatensive rats. Am J Physiol Heart Circ Physiol 2008;294:H2614–8.
[11] Kangawa K, Matsuo H. Purification and complete amino acid sequence of alpha-human atrial natriuretic polypeptide (alpha-hANP). Biochem Biophys Res Commun 1984;118:131–9.
[12] Kato J, Kobayashi K, Etoh T, Tanaka M, Kitamura K, Imamura T, et al. Plasma adrenomedullin concentration in patients with heart failure. J Clin Endocrinol Metab 1996;81:180–3.
[13] Kitamura K, Ichiki Y, Tanaka M, Kawamoto M, Emura J, Sakakibara S, et al. Immunoreactive adrenomedullin in human plasma. FEBS Lett 1994;341:288–90.
[14] Kobori H, Nangaku M, Navar LG, Nishiyama A. The intrarenal renin–angiotensin system: from physiology to the pathobiology of hypertension and kidney disease. Pharmacol Rev 2007;59:251–87.
[15] Miyata A, Kangawa K, Toshimori T, Hatoh T, Matsuo H. Molecular forms of atrial natriuretic polypeptides in mammalian tissues and plasma. Biochem Biophys Res Commun 1985;129:248–55.
[16] Miyazaki M, Okunishi H, OkamuraT, Toda N. Elevated vascular angiotensin converting enzyme in chronic two-kidney, one clip hypertension in the dog. J Hypertens 1987;5:155–60.
[17] Nagata S, Kato J, Sasaki K, Minamino N, Eto T, Kitamura K. Isolation and identification of proangiotensin-12, a possible component of the renin–angiotensin system. Biochem Biophys Res Commun 2006;350:1026–31.
[18] Oparil S, Haber E. The renin–angiotensin system (first of two parts). N Engl J Med 1974;291:389–401.
[19] Paul M, Poyan Mehr A, Kreutz R. Physiology of local renin–angiotensin systems. Physiol Rev 2006;86:747–803.
[20] Prosser HC, Forster ME, Richards AM, Pemberton CJ. Cardiac chymase converts rat proangiotensin-12 (PA12) to angiotensin II: effects of PA12 upon cardiac haemodynamics. Cardiovasc Res 2009;82:40–50.
[21] Trask AJ, Jessup JA, Chappell MC, Ferrario CM. Angiotensin-(1-12) in an alternate substrate for angiotensin peptide production in the heart. Am J Physiol Heart Circ Physiol 2008;294:H2242–7.
[22] Varagic J, Trask AJ, Jessup JA, Chappell MC, Ferrario MC. New angiotensins. J Mol Med 2008;86:663–71.

Hypertension Research (2010) 33, 374–379
 0916-9636/10 $32.00
www.nature.com/hr

ORIGINAL ARTICLE

Aldosterone antisecretagogue and antihypertensive actions of adrenomedullin in patients with primary aldosteronism

Toshihiro Kita, Mariko Tokashiki and Kazuo Kitamura

Adrenomedullin (AM) is located in the zona glomerulosa of the adrenal cortex and is considered to suppress aldosterone release. To determine the effect of AM in primary aldosteronism (PA), we infused AM (2.5 pmol kg^{-1} min^{-1}) for 27 h, followed by a 15-h recovery period, in a control group (essential hypertensives with plasma aldosterone levels ⩽100 pg ml^{-1}, n=7) and in a PA group (n=5). The control group was also infused with vehicle. Hemodynamic, hormonal, oxidative and inflammatory responses were studied. AM infusion caused similar and steady decreases in blood pressure and several markers for arteriosclerosis (for example, pulse wave velocity) in both groups. Interestingly, AM infusion suppressed aldosterone release to values within the normal range in the PA group (300.0 ± 58.4 to 111.6 ± 13.5 pg ml^{-1}, P<0.01). In the control group, aldosterone release suppression was significant but limited (81.7 ± 9.1 to 47.9 ± 9.9 pg ml^{-1}, P<0.01). The adrenocorticotropic hormone–cortisol system was not changed by AM infusion. Brain natriuretic peptide was cumulatively increased by prolonged AM infusion in both groups, probably because of cardiac overload. AM did not affect oxidative markers. In addition, a mild but significant increase in C-reactive protein (CRP) mediated by interleukin-6 was observed during AM infusion in every participant, without exception. This pathway might participate in CRP elevation in cardiovascular disease. In summary, AM seems to have an essential role in the suppression of aldosterone release in PA. AM may be an important modulator in PA, and intermediate-term (3 h) AM infusion could be used as an alternative renin-stimulating/aldosterone-suppressing test for PA detection.
Hypertension Research (2010) **33**, 374–379; doi:10.1038/hr.2010.8; published online 12 February 2010

Keywords: adrenomedullin; aldosterone; C-reactive protein; humans; primary aldosteronism

INTRODUCTION

Adrenomedullin (AM) is a potent hypotensive peptide found ubiquitously in tissues and organs, especially in cardiovascular tissues, the kidneys, lungs and endocrine glands. AM has multiple functions in a wide range of tissues and acts mainly as a vasodilatory and proliferation-inhibitory factor.[1] AM was initially identified in the adrenal medulla, but similar densities of AM were detected in the zona glomerulosa of the adrenal cortex, where AM suppresses aldosterone release.[2,3] In addition, expression of AM and its receptor was detected in Conn's adenoma cells, and AM exerted aldosterone antisecretagogue action and proliferative effects on cultured Conn's adenoma cells.[4] These findings suggest that endogenous AM may be an important modulator of aldosterone release in normal and pathogenic hyperaldosteronism. In addition, AM antagonized aldosterone-induced vascular or cardiac remodeling[5,6] and suppressed aldosterone-induced oxidative stress in a malignant hypertensive model.[7] The characteristics that define this compound, from its release to alterations in target organs, suggest that AM may be an endogenous anti-aldosterone factor, especially in the cardiovascular system.

The effects of exogenous AM administration on aldosterone release were varied in experimental animal and human studies.[8] Short-term AM administration to healthy volunteers,[9] hypertensive patients[10] and patients with renal insufficiency[11] caused vigorous stimulation of renin release, but did not change aldosterone levels; consequently, the aldosterone/renin ratio decreased. AM suppressed aldosterone levels in secondary hyperaldosteronism, such as experimental heart failure in sheep[8] or congestive heart failure in patients.[12] These data suggest that AM may be a functional antagonist of aldosterone release, but further evidence is required. We investigated the effects of AM in patients with primary aldosteronism (PA) to confirm the antagonistic effect of AM against aldosterone.

METHODS

Study subjects

Initially, essential hypertensive patients were recruited for baseline data collection for future translational research on the clinical applications of AM. After a comprehensive screening, seven hypertensive subjects who showed normal aldosterone release (plasma aldosterone ⩽100 pg ml^{-1}; control group) were

Division of Circulatory and Body Fluid Regulation, Department of Internal Medicine, Faculty of Medicine, University of Miyazaki, Miyazaki, Japan
Correspondence: Dr T Kita, Division of Circulatory and Body Fluid Regulation, Department of Internal Medicine, Faculty of Medicine, University of Miyazaki, 5200 Kihara, Kiyotake, Miyazaki 889-1692, Japan.
E-mail: t-kita@po.sphere.ne.jp
Received 16 October 2009; revised 11 December 2009; accepted 23 December 2009; published online 12 February 2010

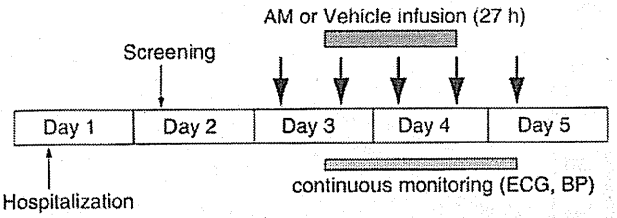

Figure 1 Experimental protocol. After a comprehensive examination of all participants, AM (2.5 pmol min^{-1} kg^{-1}) or vehicle was intravenously administered for 27 h, followed by a 15-h post-infusion period. Arrows indicate hemodynamic and blood sample assessments.

administered AM. Five patients with PA, owing to an aldosterone-producing adenoma (PA group), were then recruited to receive AM. The control group was administered vehicle after an interval of at least 1 month. All participants were admitted to our hospital and subjected to 2 days of comprehensive examinations, including urine and blood tests, chest X-ray, ECG, echocardiography, echo scan of the carotid artery and a brain MRI. Patients with narrowing or obstruction of extra- and/or intracranial major arteries, renal failure (serum creatinine >1.2 mg per 100ml), heart failure (left ventricular ejection fraction $<50\%$), coronary heart disease, peripheral artery diseases, collagen diseases or active infections were excluded. All patients with PA had cleared the diagnostic criteria for PA, as proposed by the Japan Endocrine Society (http://square.umin.ac.jp/endocrine/rinsho_juyo/index.html). Potential adrenal adenomas were confirmed by CT and/or MRI. This study was approved by the ethics committee of the institute. All participants gave their written informed consent.

Preparation of human AM

Chemically synthesized human AM was purchased from the Peptide Institute (Osaka, Japan). The homogeneity of human AM was confirmed by reverse-phase high-performance liquid chromatography and amino acid analysis. AM was dissolved in distilled water with 3.75% D-mannitol and 0.05% aminoacetic acid and then sterilized by passing through a 0.22-μm filter (Millipore, Bedford, MA, USA). The chemical nature and level of human AM in vials were verified by reverse-phase high-performance liquid chromatography. No measurable endotoxin was detected (<0.01563 EU ml^{-1}), and the material was determined to be pyrogen-free by the Japan Food Research Laboratories (Tokyo, Japan).

Study protocol

Fixed time points (0800 and 1700 hours) were assigned for comprehensive hemodynamic examination and blood sampling. Vehicle or AM administration was started at 1400 hours, as indicated in Figure 1. The comprehensive hemodynamic examination included blood pressure, heart rate (by ECG) and arteriosclerosis-related markers, such as pulse wave velocity (form PWV/ABI, BP-203RPE; Omron Colin, Komaki, Japan), augmentation index (HEM9010AI tonometer; Omron Healthcare, Kyoto, Japan) and elastic property of the carotid artery.[15] A 22-gauge cannula was inserted into the forearm vein for infusion of AM (2.5 pmol min^{-1} kg^{-1}) or vehicle diluted by 0.9% saline. Saline was administered at the rate of 5 ml h^{-1} for 27 h, followed by 15 h of recovery time. Continuous ECG monitoring and blood pressure measurements at 60-min intervals were performed throughout the experiment (Figure 1). The first urine sample was collected at around 0700 hours, before, during and after AM or vehicle administration. Plasma total and mature AM were measured using a specific immunoradiometric assay kit (Shionogi, Osaka, Japan). Plasma concentrations of other hormones, high-sensitivity C-reactive protein (CRP) and cytokines were measured using a commercially available laboratory testing service (SRL, Hachioji, Japan). Urinary concentrations of 8-isoprostane and 8-hydroxydeoxyguanosine were also measured by the laboratory testing service provided by SRL and normalized by the concentration of urinary creatinine.

Statistical analysis

All data were expressed as means ± s.e.m. Comparisons between the two groups (control *vs.* PA) were performed using the unpaired Student's *t*-test. The significance of differences was evaluated by one-factor analysis of variance with repeated measures on a time course of variables, followed by Bonferroni–Dunn *post hoc* comparison tests. A value of $P<0.05$ was the criterion for statistical significance.

Table 1 Basal characteristics

	Control	*PA*	*P-value*
Age (years)	65.3 ± 3.1	63.6 ± 2.5	NS
Sex (M/F)	7/0	3/2	
SBP (mm Hg)	154.4 ± 7.0	155.4 ± 5.8	NS
DBP (mm Hg)	93.7 ± 3.6	93.2 ± 4.5	NS
Heart rate (b.p.m.)	63.3 ± 2.8	63.6 ± 3.8	NS
PWV (cm s^{-1})	1943 ± 117	1939 ± 221	NS
Augmentation index (%)	83.7 ± 6.2	97.2 ± 4.4	NS
Elastic property (kPa)	109.7 ± 11.0	93.1 ± 7.9	NS
Aldosterone (pg ml^{-1})	81.7 ± 9.1	300 ± 58.4	0.001
Renin activity (ng ml^{-1} h^{-1})	0.90 ± 0.40	0.16 ± 0.04	NS
Adrenomedullin (fmol ml^{-1})	11.8 ± 0.6	19.2 ± 1.7	0.001
ANP (pg ml^{-1})	15.6 ± 2.8	23.4 ± 9.8	NS
BNP (pg ml^{-1})	16.6 ± 3.3	55.8 ± 36.2	NS
Noradrenaline (pg ml^{-1})	297 ± 31	384 ± 81	NS
High-sensitivity CRP (mg l^{-1})	0.78 ± 0.18	1.80 ± 0.83	0.06

Abbreviations: ANP, atrial natriuretic peptide; BNP, brain natriuretic peptide; CRP, C-reactive protein; DBP, diastolic blood pressure; NS, non-significant; PA, primary aldosteronism; PWV, pulse wave velocity; SBP, systolic blood pressure.

RESULTS

To avoid extreme rises in blood pressure, the minimal amount of Ca^{2+}-channel blocker (amlodipine 5–10 mg day^{-1}) was administered to three of seven patients in the control group and to all five patients with PA. The baseline characteristics of the control group and PA group were fairly matched, particularly with regard to age and blood pressure (Table 1). The plasma concentration of aldosterone and, interestingly, the plasma concentration of AM were increased in the PA group (Table 1).

Prolonged AM administration caused a strong and steady decrease in blood pressure; this effect was quite similar in both control and PA groups (Figure 2). Heart rate was increased by almost the same magnitude in both groups during AM administration (approximately +26% in control and +31% in PA). In addition, similar decreases in arteriosclerotic markers, such as pulse wave velocity, augmentation index and elastic property of the carotid artery, were accompanied by reductions in blood pressure in both groups (Figure 2). These effects returned to baseline after a 15-h interval. Harmful symptoms or reactions were not observed in any of the participants.

As indicated in Figure 3, AM administration caused significant increases in total AM (approximately 3.1-fold in the control group and 2.1-fold in the PA group). Peak concentrations of AM were comparable in both groups. Plasma concentration of mature AM also increased: approximately 6.7-fold in both groups (Table 2). Most interestingly, AM administration caused strong and significant suppression of aldosterone release in the PA group; levels reached the normal range (111.6 ± 13.5 pg ml^{-1}) at the end of AM infusion (Figure 3). Significant but moderate suppression of aldosterone release was also observed in the control group during AM administration. AM infusion stimulated renin release in the control group, but this change was not significant. A very small but significant increase in renin was observed in the PA group (Figure 3). Standard renin-secretion stimulating tests (captopril loading and furosemide loading+walking) did not increase renin levels in the PA group (data not shown).

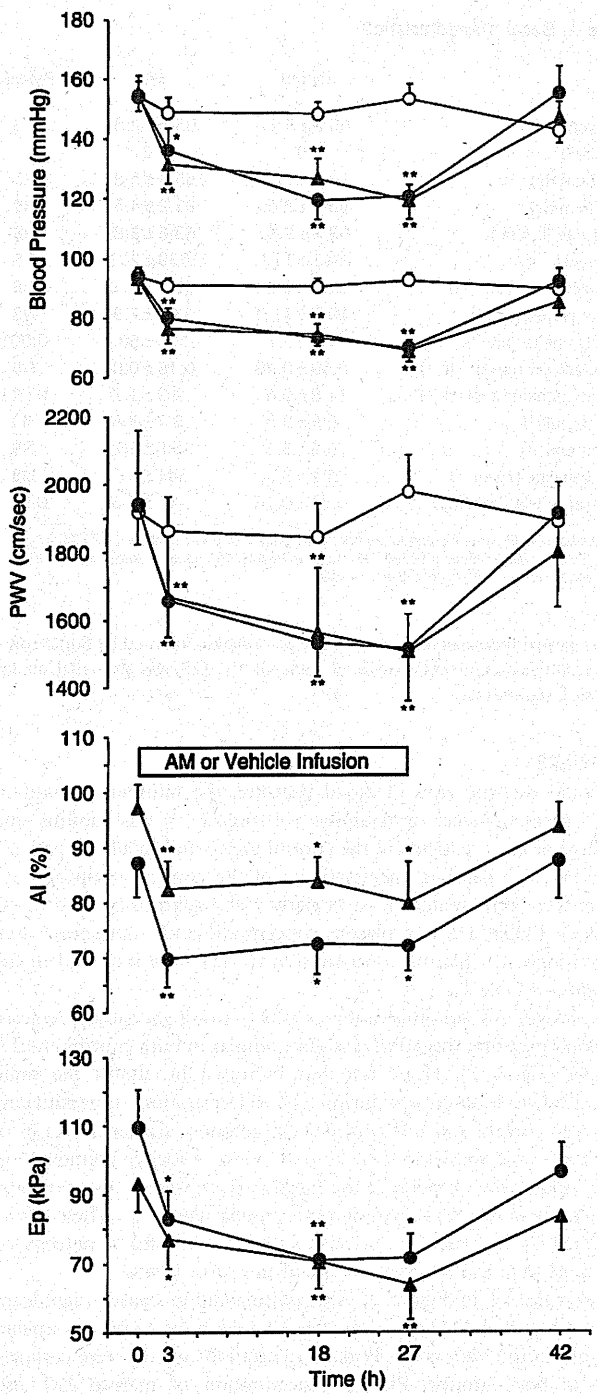

Figure 2 Changes in blood pressure, pulse wave velocity (PWV), augmentation index (AI) and elastic property (Ep) of the carotid artery during infusion of adrenomedullin (●: control group, ▲: PA group) or vehicle (○: control group). Data are means ± s.e.m. *$P<0.05$, **$P<0.01$, each *vs.* baseline.

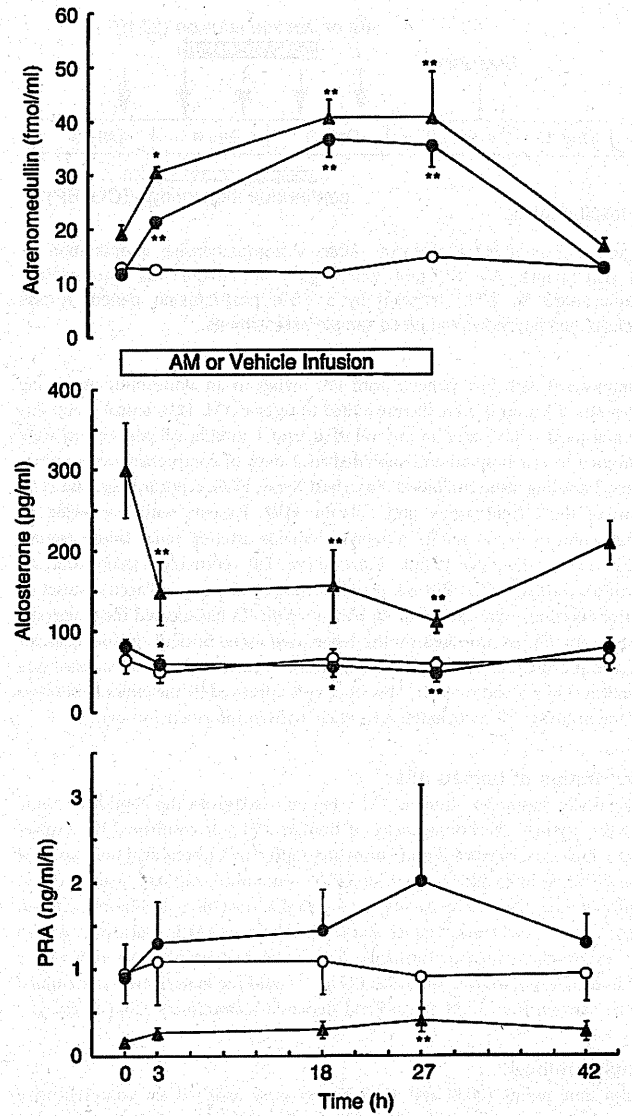

Figure 3 Changes in the plasma concentration of adrenomedullin, aldosterone and plasma renin activity (PRA) during infusion of adrenomedullin (●: control group, ▲: PA group) or vehicle (○: control group). Data are means ± s.e.m. *$P<0.05$, **$P<0.01$, each *vs.* baseline.

Other hormonal changes are summarized in Table 2. Levels of cAMP, the second messenger of AM, were unchanged in both groups. An increase in atrial natriuretic peptide (ANP) level, accompanied by a cGMP increase, was only observed in the PA group during AM administration. Brain natriuretic peptide (BNP) level was increased in both groups in a late phase of the experiment, but this alteration was not associated with the cGMP increase. It is noteworthy that AM did not affect the adrenocorticotropic hormone–cortisol system in either group.

To evaluate the acute effects of AM on oxidative stress and the immune system, we assessed oxidative stress markers, cytokines and high-sensitivity CRP. Basal levels of CRP were below the normal range ($<0.3\,mg\,dl^{-1}$) in all participants, and the average value was $0.12 \pm 0.04\,mg\,dl^{-1}$. AM administration did not affect the oxidative stress markers (8-isoprostane and 8-hydroxydeoxyguanosine) in either group (Table 2). Surprisingly, AM administration induced expression of interleukin-6 (IL-6), which was followed by an increase in CRP. This reaction was confirmed in every participant, without exception. All results are summarized in Figure 4. (The unit for CRP is $mg\,l^{-1}$.)

Table 2 Changes of parameters in blood and urine tests

	Before	*3 h*	*18 h*	*27 h*	*Recovery*
Total protein, g dl^{-1}					
Vehicle	6.7±0.1		6.7±0.1		6.7±0.1
Cnt-AM	7.1±0.2		6.8±0.1		7.2±0.2
PA-AM	7.2±0.1		6.6±0.2*		7.1±0.3
Mature adrenomedullin, fmol ml^{-1}					
Vehicle	2.4±0.1	3.2±0.9	2.7±0.6	3.1±0.7	2.3±0.2
Cnt-AM	2.0±0.4	8.1±1.1**	13.4±1.8**	11.8±2.6**	1.6±0.3
PA-AM	2.8±0.4	9.6±2.0*	18.8±3.5**	12.2±2.4*	2.8±0.8
Noradrenaline, pg ml^{-1}					
Vehicle	226±35	290±52	219±29	242±27	219±25
Cnt-AM	297±31	336±21	374±30	316±25	341±55
PA-AM	384±81	428±110	487±146	469±122	417±99
cAMP, pmol ml^{-1}					
Vehicle	11.7±0.7	11.3±0.7	12.5±1.0	12.4±0.4	12.4±0.8
Cnt-AM	14.4±0.8	15.1±0.6	15.6±0.8	14.9±0.9	14.0±0.6
PA-AM	13.2±1.0	14.6±1.1	13.8±1.1	13.6±1.0	12.5±1.4
cGMP, pmol ml^{-1}					
Vehicle	4.5±0.7	3.5±0.8	3.2±0.4	3.9±0.5	3.3±0.3
Cnt-AM	3.4±0.3	3.9±0.5	4.5±0.8	3.6±0.4	3.3±0.2
PA-AM	2.6±0.4	4.7±0.5**	3.6±0.3*	4.4±0.6**	2.7±0.3
ANP, pg ml^{-1}					
Vehicle	23.6±4.1	19.6±2.0	17.0±1.6	20.9±1.5	17.1±1.6
Cnt-AM	15.6±2.8	23.9±6.8	29.6±7.4	29.6±9.1	18.6±4.4
PA-AM	23.4±9.8	40.0±12.0*	41.0±7.6*	49.8±9.2**	29.0±10.4
BNP, pg ml^{-1}					
Vehicle	18.9±5.0	17.7±4.4	15.1±3.3	13.2±2.9	10.6±2.1
Cnt-AM	16.6±3.3	12.7±2.8	31.1±7.4	61.1±15.2**	53.0±12.4**
PA-AM	55.8±36.2	42.9±24.8	79.8±37.6	131.3±53.5*	115.7±56.3*
ACTH, pg ml^{-1}					
Vehicle	26.0±5.9		21.7±3.6		22.3±3.8
Cnt-AM	20.6±1.9		18.7±5.3		22.1±3.2
PA-AM	18.5±2.8		18.2±3.9		20.6±5.9
Cortisol, μg dl^{-1}					
Vehicle	8.4±0.5		11.2±1.6		11.9±1.3
Cnt-AM	10.7±1.2		14.9±2.5		13.2±1.6
PA-AM	16.7±3.6		17.8±4.6		15.6±1.9
8-Isoprostane, pg per mg creatinine					
Vehicle	256±62		169±23		237±60
Cnt-AM	197±25		206±25		168±19
PA-AM	207±41		252±46		253±54
8-OHdG, ng per mg creatinine					
Vehicle	10.1±1.3		10.1±1.3		9.6±1.1
Cnt-AM	7.8±1.6		7.6±0.9		7.7±0.5
PA-AM	11.9±5.1		9.4±2.0		12.5±2.9

Abbreviations: ACTH, adrenocorticotropic hormone; ANP, atrial natriuretic peptide; BNP, brain natriuretic peptide; Cnt-AM, control group with adrenomedullin infusion; 8-OHdG, 8-hydroxydeoxyguanosine; PA, primary aldosteronism group.
*P<0.05, **P<0.01 *vs.* before.

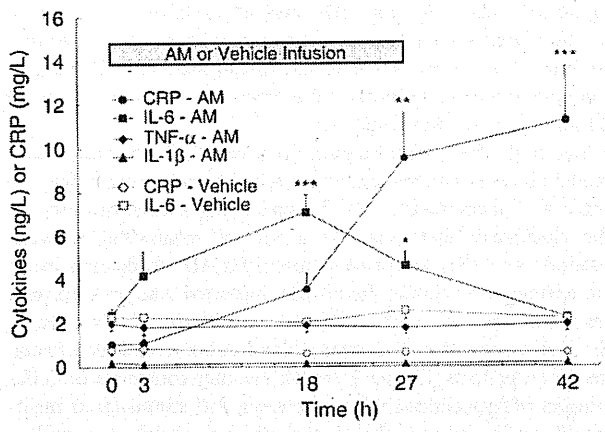

Figure 4 Changes in the serum concentration of cytokines and high-sensitivity CRP during infusion of adrenomedullin or vehicle. Data are summarized for all participants (control+PA group, n=12) and expressed as means±s.e.m. *P<0.05, **P<0.01, ***P<0.0001, each *vs.* baseline. Abbreviations: IL-1β, interleukin-1β (high sensitivity); IL-6, interleukin-6; TNF-α, tumor necrosis factor-α (high sensitivity).

DISCUSSION

This is the only study to investigate long-term administration (over 24 h) of AM in humans.[14] The study put considerable strain on the participants, and hence the minimum number of participants required to achieve statistical significance was considered. Prolonged infusion of AM caused a hypotensive reaction, accompanied by improvements in arteriosclerotic markers (pulse wave velocity, augmentation index and elastic property of the carotid artery) in both the control group, with normal aldosterone levels, and in patients with PA. More importantly, we confirmed for the first time that AM infusion suppressed aldosterone release, producing a normal range in patients with PA.

AM is located in the zona glomerulosa of the adrenal cortex and Conn's adenoma.[2–4] AM has a direct inhibitory effect on aldosterone release from adrenocortical cells and Conn's adenoma cells.[15] Previous human experiments have produced varied results on the effects of intravenous infusion of AM on aldosterone release.[8–12] Our study showed that suppression of aldosterone release by AM in the control group was significant but quite limited (Figure 3). A hypotensive reaction due to AM infusion was observed over a wide dosage range, but the suppressive effect of AM on aldosterone release was time and dose dependent, suggesting that there may be relatively high thresholds for suppression.[8,16] We used a 'moderate' amount of AM (2.5 pmol kg^{-1} min^{-1} or 15 ng kg^{-1} min^{-1}), which led to a significant decrease in aldosterone release after 3 h of infusion (Figure 3). In a previous report, a similar amount of AM (16 ng kg^{-1} min^{-1}), infused for 2 h, did not change renin or aldosterone release in healthy volunteers.[9] The dose of AM was increased to 32 ng kg^{-1} min^{-1} and infusion was continued for another 2 h: a vigorous increase in renin release was reported, but there were no changes in aldosterone.[9] A large dose of AM infusion caused strong hypotension and strongly stimulated renin release as well as sympathetic nervous activity.[8] This may have interfered with the suppressive effect on aldosterone release. AM administration stimulates renin release.[8–12] On the other hand, AM can partially, but not completely, suppress increases in aldosterone induced by angiotensin II in humans.[17] In PA patients, renin activity is extremely suppressed, suggesting that AM could mediate essential aldosterone suppression. Under the conditions studied here

(2.5 pmol kg^{-1} min^{-1} for 3 h), AM may be useful as an alternative renin-stimulating (and aldosterone-suppressing) test for PA detection. In addition, it is important to elucidate the suppressive mechanism of AM because the lower aldosterone concentration in blood that results could benefit the cardiovascular system.

In this study, the plasma concentration of AM in PA patients was increased (Table 1). We and one other research group have previously reported this phenomenon.[18,19] The underlying mechanism remains to be elucidated: there may be a mutual relationship between aldosterone and AM. Aldosterone stimulates AM production in rat aortic adventitia or cardiac fibroblasts; increased AM, in turn, regulates the proliferative action of aldosterone in those cells.[5,6] Increased levels of AM were able to suppress blood pressure and aldosterone release in PA patients (Figures 2 and 3). AM may counteract or buffer the impact of hyperaldosteronism; however, AM stimulates or maintains cell proliferation in the adrenal zona glomerulosa as well as Conn's adenoma cells.[4,20,21] Letizia *et al.*[19] reported that the plasma level of AM was positively related to the tumor size of the adenoma in PA. It is highly probable that AM modulates the pathophysiological condition of PA, but further study is required to elucidate the participation of AM in PA.

AM administration caused several alterations in the humoral factors measured (Table 2). In particular, ANP was significantly increased, accompanied by continuous increases in cGMP, but only in PA patients. AM did not affect ANP or BNP levels in normal subjects or in patients with hypertension or heart failure.[9,10,12] The ANP-stimulating effect in PA patients is interesting, although the mechanism is unclear. ANP inhibits aldosterone secretion and is considered to be a key factor in aldosterone escape (or aldosterone breakthrough).[22,23] Thus, increased ANP may participate in the suppression of aldosterone release in PA. However, aldosterone-producing adenomas do not have a receptor for ANP and ANP did not suppress aldosterone release from the adenoma.[24] In addition, ANP infusion did not suppress aldosterone release in patients with PA.[25] The AM-induced ANP increase does not seem to be related to aldosterone suppression in PA by AM. ANP increased during AM infusion, whereas BNP was increased in both groups during the late phase of the experiment (Table 2). AM has a cAMP-dependent and -independent positive inotropic effect on myocardium.[26,27] In addition to the decrease in cardiac afterload induced by vasodilation, cardiac output was markedly increased by AM administration.[9–12] The cumulative increase in BNP may reflect cardiac overload induced by prolonged infusion of AM. Although none of the participants experienced adverse events, cardiac overload must be carefully avoided during longer term application of AM. AM has diuretic and natriuretic effects,[10–12] and AM administration increased ANP and BNP levels in this study; however, we did not study the diuretic and natriuretic effects of these factors. Participants would not agree to use an additional balloon catheter for accurate urine collection. Total saline infusion was only 135 ml over 27 h, so it should not have influenced urine samples in this experiment. Because total protein was decreased after AM administration (Table 2), significant decreases were measured in PA patients, while serum levels of sodium were not altered (control: 141.1 ± 1.1, 141.4 ± 0.8 and 140.9 ± 0.8 mEq l^{-1}; PA: 143.6 ± 0.5, 144.4 ± 0.5 and 143.4 ± 0.4 mEq l^{-1} before, during and after AM administration, respectively). The decreases in total protein may be due to vasodilation induced by AM. Decreases in hematocrit have been previously reported,[28] suggesting some hemodilution.

This is the first report suggesting that prolonged administration of AM can induce CRP production through IL-6 in humans. AM is known to inhibit strong inflammation, such as sepsis.[29] However, AM can exert both pro-inflammatory and anti-inflammatory effects, and it stimulates IL-6 production in macrophages.[30] As yet, there are no data on the effect of AM on CRP production in humans who do not exhibit accelerated inflammation. The time course of IL-6 and CRP changes (Figure 4) and the close relationship between both factors (relationship between maximum changes of CRP and IL-6; $r=0.64$, $P=0.034$) in the present study strongly suggest an interaction of IL-6 with CRP. Isumi *et al.*[31] reported that the stimulatory effect of AM on *IL-6* gene transcription took place immediately, reached a plateau within 30 min, and then decreased gradually. The short-term increase in IL-6 in the present study is compatible with the acute-phase stimulant nature of AM. However, IL-6 is a key factor in the regulation of CRP production in the liver, the main source of serum CRP.[31] As CRP has a higher rate of increase and longer half-life (about 19 h) in comparison with IL-6 or AM,[32] the extended increase in CRP observed in this study was not unexpected.

In addition to modulating the vascular tonus, AM influences the progression of atherosclerosis[1] and stimulates production of IL-6.[30] Moreover, AM and inflammatory markers, such as IL-6 and CRP, are elevated in patients with hypertension, CHD and peripheral artery disease: positive correlations between AM and IL-6 or CRP[1,33] have been reported. AM production is most likely stimulated in the vasculature, as a reaction to a variety of stress-related factors, including hormones, mechanical stresses, metabolic factors and cytokines.[34] In addition to inflammation, many kinds of stimuli to blood vessels would influence AM levels and consequently CRP. Although AM is merely one factor regulating CRP production, this intimate relationship of AM with CRP via IL-6 may represent a pivotal role for AM in a mechanism linking serum CRP and vascular alterations. However, prolonged elevation of AM in PA patients did not completely correlate with CRP elevation in PA patients (Table 1). Further studies to confirm the roles of AM in the regulation of CRP levels under various conditions are required.

In conclusion, we have shown that prolonged administration of AM can normalize blood pressure and aldosterone release in PA. The ability of AM to suppress autonomous release of aldosterone in PA seems to be substantial when compared with the suppressive properties of ANP in PA that are unrelated to aldosterone. AM may be an important modulator in PA, and AM seems to be a unique tool and potential target for research into aldosterone release in PA. In addition, AM mildly stimulates CRP production at baseline, through IL-6 or non-stimulated inflammatory conditions in humans. This pathway might participate in CRP elevation in cardiovascular disease.

CONFLICT OF INTEREST

The authors declare no conflict of interest.

ACKNOWLEDGEMENTS

This study was supported in part by Health and Labor Science Research Grants for Translational Research from the Ministry of Health, Labor and Welfare, Japan.

1 Eto T, Kato J, Kitamura K. Regulation of production and secretion of adrenomedullin in the cardiovascular system. *Regul Pept* 2002; **112**: 61–69.
2 Kapas S, Martínez A, Cuttitta F, Hinson JP. Local production and action of adrenomedullin in the rat adrenal zona glomerulosa. *J Endocrinol* 1998; **156**: 477–484.
3 Mazzocchi G, Albertin G, Andreis PG, Neri G, Malendowicz LK, Champion HC, Bahçelioglu M, Kadowitz PJ, Nussdorfer GG. Distribution, functional role, and signaling mechanism of adrenomedullin receptors in the rat adrenal gland. *Peptides* 1999; **20**: 1479–1487.

4 Forneris M, Gottardo L, Albertin G, Malendowicz LK, Nussdorfer GG. Expression and function of adrenomedullin and its receptors in Conn's adenoma cells. *Int J Mol Med* 2001; **8**: 675–679.
5 Jiang W, Yang JH, Pan CS, Qi YF, Pang YZ, Tang CS. Effects of adrenomedullin on cell proliferation in rat adventitia induced by aldosterone. *J Hypertens* 2004; **22**: 1953–1961.
6 Jiang W, Yang JH, Wang SH, Pan CS, Qi YF, Zhao J, Tang CS. Effects of adrenomedullin on aldosterone-induced cell proliferation in rat cardiac fibroblasts. *Biochim Biophys Acta* 2004; **1690**: 265–275.
7 Rahman M, Nishiyama A, Guo P, Nagai Y, Zhang GX, Fujisawa Y, Fan YY, Kimura S, Hosomi N, Omori K, Abe Y, Kohno M. Effects of adrenomedullin on cardiac oxidative stress and collagen accumulation in aldosterone-dependent malignant hypertensive rats. *J Pharmacol Exp Ther* 2006; **318**: 1323–1329.
8 Charles CJ, Lainchbury JG, Nicholls MG, Rademaker MT, Richards AM, Troughton RW. Adrenomedullin and the renin-angiotensin-aldosterone system. *Regul Pept* 2003; **112**: 41–49.
9 Lainchbury JG, Troughton RW, Lewis LK, Yandle TG, Richards AM, Nicholls MG. Hemodynamic, hormonal, and renal effects of short-term adrenomedullin infusion in healthy volunteers. *J Clin Endocrinol Metab* 2000; **85**: 1016–1020.
10 Troughton RW, Levis LK, Yandle TG, Richards AM, Nicholls MG. Hemodynamic, hormone, and urinary effects of adrenomedullin infusion in essential hypertension. *Hypertension* 2000; **36**: 588–593.
11 McGregor DO, Troughton RW, Frampton C, Lynn KL, Yandle T, Richards AM, Nicolls MG. Hypotensive and natriuretic actions of adrenomedullin in subjects with chronic renal impairment. *Hypertension* 2001; **37**: 1279–1284.
12 Nagaya N, Satoh T, Nishikimi T, Uematsu M, Furuichi S, Sakamaki F, Oya H, Kyotani S, Nakanishi N, Goto Y, Masuda Y, Miyatake K, Kangawa K. Hemodynamic, renal, and hormonal effects of adrenomedullin infusion in patients with congestive heart failure. *Circulation* 2000; **101**: 498–503.
13 Blankenhorn DH, Chin HP, Conover DJ, Nessim SA. Ultrasound observation on pulsation in human carotid artery lesions. *Ultrasound Med Biol* 1988; **14**: 583–587.
14 Nishikimi T, Karasawa T, Inaba C, Ishimura K, Tadokoro K, Koshikawa S, Yoshihara F, Nagaya N, Sakio H, Kangawa K, Matsuoka H. Effects of long-term intravenous administration of adrenomedullin (AM) plus hANP therapy in acute decompensated heart failure: a pilot study. *Circ J* 2009; **73**: 892–898.
15 Andreis PG, Tortorella C, Mazzocchi G, Nussdorfer GG. Proadrenomedullin N-terminal 20 peptide inhibits aldosterone secretion of human adrenocortical and Conn's adenoma cells: comparison with adrenomedullin effect. *J Clin Endocrinol Metab* 1998; **83**: 253–257.
16 Troughton RW, Frampton CM, Levis LK, Yandle TG, Richards AM, Nicholls MG. Differing thresholds for modulatory effects of adrenomedullin infusion on haemodynamic and hormone responses to angiotensin II and adrenocorticotrophic hormone in healthy volunteers. *Clin Sci (Lond)* 2001; **101**: 103–109.
17 Petrie MC, Hillier C, Morton JJ, McMurray JJV. Adrenomedullin selectively inhibits angiotensin II-induced aldosterone secretion in humans. *J Hypertens* 2000; **18**: 61–64.
18 Kato J, Kitamura K, Kuwasako K, Tanaka M, Ishiyama Y, Shimokubo T, Ichiki Y, Nakamura S, Kangawa K, Eto T. Plasma adrenomedullin in patients with primary aldosteronism. *Am J Hypertens* 1995; **8**: 997–1000.
19 Letizia C, De Toma G, Cerci S, Massa R, Coassin S, Subioli S, Scuro L, De Ciocchis A. Adrenomedullin levels are high in primary aldosteronism due to adenoma and decline after surgical cure. *Blood Press* 1998; **7**: 19–23.
20 Andreis PG, Albertin G, Conconi MT, Carraro G, Malendowicz LK, Ziolkowska A, Nussdorfer GG. Evidence for an autocrine-paracrine role of adrenomedullin in the cultured rat adrenal zona glomerulosa cells. *Int J Mol Med* 2002; **10**: 401–405.
21 Rossi GP, Conconi MT, Malendowicz LK, Nussdorfer GG. Role of the endogenous adrenomedullin system in regulating the secretion and growth of rat adrenal cortex. *Hypertens Res* 2003; **26** (Suppl): S85–S92.
22 Ganquly A. Atrial natriuretic peptide-induced inhibition of aldosterone secretion: a quest for mediator(s). *Am J Physiol* 1992; **263**: E181–E194.
23 Yokota N, Bruneau BG, Kuroski de Bold ML, de Bold AJ. Atrial natriuretic factor significantly contributes to the mineralocorticoid escape phenomenon. Evidence for a guanylate cyclase-mediated pathway. *J Clin Invest* 1994; **94**: 1938–1946.
24 Shionoiri H, Hirawa N, Takasaki I, Ishikawa Y, Oda H, Minamisawa K, Sugimoto K, Matsukawa T, Ueda S, Miyajima E. Functional atrial natriuretic peptide receptor in human adrenal tumor. *J Cardiovasc Pharmacol* 1989; **13** (Suppl 6): S9–S12.
25 Rocco S, Opocher G, Carpenè G, Mantero F. Atrial natriuretic peptide infusion in primary aldosteronism. Renal, hemodynamic and hormonal effects. *Am J Hypertens* 1990; **3**: 668–673.
26 Ihara T, Ikeda U, Tate Y, Ishibashi S, Shimada K. Positive inotropic effects of adrenomedullin on rat papillary muscle. *Eur J Pharmacol* 2000; **390**: 167–172.
27 Szokodi I, Kinnunen P, Tavi P, Weckstrom M, Toth M, Ruskoaho H. Evidence for cAMP-independent mechanisms mediating the effects of adrenomedullin, a new inotropic peptide. *Circulation* 1998; **97**: 1062–1070.
28 Rademaker MT, Charles CJ, Espiner EA, Nicholls MG, Richards AM. Long-term adrenomedullin administration in experimental heart failure. *Hypertension* 2002; **40**: 667–672.
29 Yang S, Zhou M, Fowler DE, Wang P. Mechanisms of the beneficial effect of adrenomedullin and adrenomedullin-binding protein-1 in sepsis: down-regulation of proinflammatory cytokines. *Crit Care Med* 2002; **30**: 2729–2735.
30 Wong LYF, Cheung BMY, Li Y-Y, Tang F. Adrenomedullin is both proinflammatory and anti-inflammatory: its effects on gene expression and secretion of cytokines and macrophage migration inhibitory factor in NR8383 macrophage cell line. *Endocrinology* 2005; **146**: 1321–1327.
31 Isumi Y, Minamino N, Kubo A, Nishimoto N, Yoshizaki K, Yoshioka M, Kangawa K, Matsuo H. Adrenomedullin stimulates interleukin-6 production in Swiss 3T3 cells. *Biochem Biophys Res Commun* 1998; **244**: 325–331.
32 Pepys MB, Hirschfield GM. C-reactive protein: a critical update. *J Clin Invest* 2003; **111**: 1805–1812.
33 Suzuki Y, Horio T, Nonogi H, Hayashi T, Kitamura K, Eto T, Kangawa K, Kawano Y. Adrenomedullin as a sensitive marker for coronary and peripheral arterial complications in patients with atherosclerotic risks. *Peptides* 2004; **25**: 1321–1326.
34 Kato J, Tsuruda T, Kita T, Kitamura K, Eto T. Adrenomedullin: a protective factor for blood vessels. *Arterioscler Thromb Vasc Biol* 2005; **25**: 2480–2487.

Reciprocal Contribution of Pentraxin 3 and C-Reactive Protein to Obesity and Metabolic Syndrome

Tsuneo Ogawa[1], Yurika Kawano[2], Takuroh Imamura[2], Kumiko Kawakita[1], Mina Sagara[3], Takeshi Matsuo[4], Yousuke Kakitsubata[5], Tadashi Ishikawa[4], Kazuo Kitamura[2], Kinta Hatakeyama[6], Yujiro Asada[6] and Tatsuhiko Kodama[7]

Pentraxin 3 (PTX3) is an acute-phase protein that shares structural homology with C-reactive protein (CRP). PTX3 is produced in macrophages, endothelial cells, and adipocytes in response to inflammatory stimuli, whereas hepatocytes are the main source of CRP. Because obesity and metabolic syndrome (MetS) are considered chronic inflammatory states, PTX3 might be involved in the pathogenesis of obesity and MetS as well as CRP. Levels of CRP correlated positively with body weight, BMI, waist circumference (WC), fasting plasma glucose and interleukin (IL)-6, and negatively with high-density lipoprotein cholesterol and adiponectin in healthy males. In contrast, PTX3 correlated positively with adiponectin, and negatively with body weight, BMI, WC, and triglyceride. Plasma CRP significantly increased, whereas plasma PTX3 significantly decreased with increasing BMI. Plasma CRP and PTX3 levels were significantly higher and lower, respectively, in individuals who had more than one MetS component compared with those who had none. In conclusion, PTX3 and CRP antagonistically participate in the development of obesity or MetS.

Obesity (2010) **18**, 1871–1874. doi:10.1038/oby.2009.507

Obesity and metabolic syndrome (MetS) should be considered as chronic inflammatory states. C-reactive protein (CRP) belongs to the pentraxin family and it is a plasma marker of acute and chronic inflammation. It is mainly produced in the liver in response to inflammatory mediators, particularly interleukin (IL)-6 (ref. 1). Levels of CRP are elevated in obese persons, and can predict future cardiovascular risks (2). Pentraxin 3 (PTX3) is structurally related to other proteins of the pentraxin family but it is distinct from the classical pentraxins such as CRP (3). Various cells including macrophages, endothelial cells, smooth muscle cells, white blood cells, and adipocytes produce PTX3 in response to inflammatory cytokines such as IL-1 and tumor necrosis-α (4–7). Plasma PTX3 levels are positively associated with adhesion molecules and endothelial dysfunction in patients with chronic kidney disease (8,9), and rapidly increase in patients with acute coronary syndrome (10,11). However, the relationship between PTX3 and chronic inflammatory states such as obesity or MetS remains unknown. Because different cells within adipose tissue might produce PTX3 (7), it could be a more sensitive marker of inflammation caused by obesity and MetS than CRP. Here, we examined plasma PTX3 levels in 226 nonmedicated, healthy males to assess relationships between PTX3 and BMI as well as MetS components.

METHODS AND PROCEDURES

Participants

We enrolled 226 apparently healthy males (range 26–82 years) who presented at a public health center associated with Miyazaki Social Insurance Hospital for an annual routine health check and who provided written informed consent to participate in the study. None of them were under medication including nonsteroidal anti-inflammatory drugs and other over-the-counter drugs such as aspirin. We measured height, body weight, waist circumference (WC), blood pressure, and blood parameters. Smoking status was scored based on numbers of cigarettes smoked per day as: nonsmoker, 0; 1–9 cigarettes, 1; 10–19 cigarettes, 2; and ≥20 cigarettes, 3. The participants were assigned to group 1, 2, 3, or 4 based on BMI of 18–22; 22–25; 25–28, and 28–43, respectively. The participants were also classified according to the number of MetS components as follows: (i) none, (ii) one, (iii) two, and (iv) three or four. The MetS components were defined as: (i) WC of ≥85 cm measured at the level of the navel, (ii) systolic blood pressure ≥130 mm Hg or diastolic blood pressure ≥85 mm Hg, (iii) triglyceride ≥150 mg/dl or high-density lipoprotein cholesterol (HDL-C) <40 mg/dl, and (iv) fasting plasma glucose ≥110 mg/dl. The Ethical Committee of Miyazaki Social Insurance Hospital approved the study.

[1]Department of Nutrition Management, Minami Kyushu University, Miyazaki, Japan; [2]First Department of Internal Medicine, University of Miyazaki, Miyazaki, Japan; [3]Perseus Proteomics Inc., Tokyo, Japan; [4]Department of Internal Medicine, Miyazaki Social Insurance Hospital, Miyazaki, Japan; [5]Public Health Center, Miyazaki Social Insurance Hospital, Miyazaki, Japan; [6]Department of Pathology, University of Miyazaki, Miyazaki, Japan; [7]Research Center for Advanced Science and Technology, University of Tokyo, Tokyo, Japan. Correspondence: Takuroh Imamura (imatak@med.miyazaki-u.ac.jp)

Received 15 April 2009; accepted 28 December 2009; published online 28 January 2010. doi:10.1038/oby.2009.507

Assays

Plasma levels of tumor necrosis-α (intra- and interassay coefficients of variation (CVs), 5.2 and 7.3%, respectively), adiponectin (intra- and interassay CV, 4.7 and 6.8%, respectively), and IL-6 (intra- and interassay CV, 4.2 and 6.4%, respectively) were determined using ELISA kits from R&D Systems (Minneapolis, MN). Plasma levels of IL-1β (intra- and interassay CV, 10.0 and 12.0%, respectively) and PTX3 (intra- and interassay CV, 4.1 and 4.3%, respectively) were determined using ELISA kits from RayBiotech (Norcross, GA) and Perseus Proteomics (Tokyo, Japan), respectively. Details of the PTX3 assay including the detection limit have already been published (10). Plasma CRP levels (intra- and interassay CV, 1.3 and 2.8%, respectively) were measured using high-sensitivity assays (Denka Seiken, Japan). All other plasma data were conventionally measured at Miyazaki Social Insurance Hospital.

Statistical analyses

All results are expressed as means ± s.e.m. We determined statistical differences among multiple groups using ANOVA, and pairwise differences between two groups using the Bonferroni test. Multiple groups were compared using analysis of covariance when adjustment for BMI was required. Relationships between CRP or PTX3 and other variables were determined by multiple regression analysis to adjust for age and smoking status. The normality of distribution for each parameter was confirmed using the Shapiro–Wilk analysis. All statistical calculations were performed using the Excel Tokei software series (Esumi, Tokyo, Japan.).

RESULTS

Characteristics of the participants

Table 1 shows the anthropological, clinical, and biochemical features of the participants.

Table 1 Clinical and biochemical characteristics of subjects

Parameter	Means ± s.d.
Age (years)	48.0 ± 9.6
BW (kg)	73.4 ± 12.5
Height (cm)	170.4 ± 6.4
BMI (kg/m²)	25.2 ± 3.8
WC (cm)	88.4 ± 9.5
SBP (mm Hg)	121 ± 18
DBP (mm Hg)	78 ± 12
T-CHO (mg/dl)	208 ± 35
HDL-C (mg/dl)	55 ± 12
TG (mg/dl)	165 ± 166
FPG (mg/dl)	102 ± 27
TNF-α (pg/ml)	0.88 ± 0.58
Adiponectin (μg/ml)	4.03 ± 2.86
IL-6 (pg/ml)	1.74 ± 1.58
IL-1β (pg/ml)	1.61 ± 1.66
CRP (mg/dl)	0.12 ± 0.17
PTX3 (ng/ml)	1.79 ± 0.89

BW, body weight; CRP, C-reactive protein; DBP, diastolic blood pressure; FPG, fasting plasma glucose; HDL-C, high-density lipoprotein cholesterol; IL, interleukin; PTX3, pentraxin 3; SBP, systolic blood pressure; T-CHO, total cholesterol; TG, triglyceride; TNF-α, tumor necrosis factor-α; WC, waist circumference.

Relationships between CRP or PTX3 and other parameters

Plasma CRP correlated positively with body weight, BMI, WC, fasting plasma glucose, and IL-6, and negatively with HDL-C and adiponectin levels after adjustment for age and smoking status. On the other hand, plasma PTX3 correlated positively with adiponectin and negatively with BMI, WC, and triglyceride (**Table 2**).

Plasma PTX3, CRP, adiponectin, and IL-6 levels among BMI groups

The numbers of individuals in groups 1, 2, 3, and 4 classified according to BMI were 39, 76, 65, and 46, respectively. Plasma CRP ($P < 0.05$) and IL-6 ($P < 0.05$) levels significantly increased with increasing BMI, whereas plasma PTX3 ($P < 0.01$) and adiponectin ($P < 0.01$) levels significantly decreased with increasing BMI (**Figure 1**).

Plasma PTX3, CRP, adiponectin, and IL-6 among groups classified by the number of MetS components

The numbers of individuals with none (Control), one (group 1), two (group 2) and three or four (group 3) MetS components were 40, 65, 80, and 41, respectively. Plasma PTX3 levels in groups 1 (1.63 ± 0.09 ng/ml), 2 (1.73 ± 0.10 ng/ml), and 3 (1.68 ± 0.09 ng/ml) were significantly lower than control values (2.29 ± 0.19 ng/ml) ($P < 0.01$). However, groups 1, 2, and 3 did not significantly differ. The differences in plasma PTX3 between the control group and groups with Mets components persisted even after adjustment for BMI. Likewise, plasma adiponectin levels in groups 1 (4.21 ± 0.37 μg/ml), 2 (3.42 ± 0.24 μg/ml), and 3 (2.88 ± 0.25 μg/ml) did not significantly differ but were all significantly lower than those of the Control group (6.16 ± 0.58 μg/ml; $P < 0.01$). On the other hand, plasma CRP levels in groups 1 (0.119 ± 0.016 mg/dl), 2 (0.124 ± 0.017 mg/dl), and 3 (0.120 ± 0.018 mg/dl) did not significantly differ, but were significantly higher than those of the Control (0.071 ± 0.021 mg/dl; $P < 0.05$). Plasma IL-6 and CRP levels were similar (data not shown).

DISCUSSION

CRP is mainly produced in hepatocytes in response to IL-6, whereas various types of cells including adipocytes locally and directly produce PTX3 (4,7,12). Given the cellular sources of PTX3 and the components of adipose tissue, we postulated that the PTX3 level would increase with chronic inflammation caused by obesity and MetS. However, the present findings suggested that PTX3 and CRP are inversely involved in obesity and MetS, which contradicted this hypothesis. An inverse relationship between plasma PTX3 and BMI in healthy individuals (13), patients with chronic kidney disease (9) and those on hemodialysis (14) has recently been reported. Malnutrition is also associated with an increased plasma PTX3 level in patients with chronic kidney disease (8) and in those on hemodialysis (14). Bosutti *et al.* demonstrated that plasma PTX3 levels inversely correlate with fat mass and that less body fat means decreased and increased plasma levels of CRP and PTX3, respectively (15). Our findings of reciprocal changes

Table 2 Correlations between CRP and PTX3 and other factors after adjustment for age and smoking status

	CRP		PTX3	
	Coefficient	*P* value	Coefficient	*P* value
BW	0.1766	0.0096†	−0.1693	0.0120*
Height	−0.0458	0.5420	−0.0355	0.6325
BMI	0.2079	0.0018†	−0.1628	0.0139*
WC	0.2238	0.0008†	−0.1706	0.0099†
SBP	0.0412	0.5632	−0.0621	0.3777
DBP	0.1288	0.0593	−0.0879	0.1935
T-CHO	0.0765	0.2538	−0.0946	0.1527
HDL-C	−0.1426	0.0348*	0.1089	0.1034
TG	−0.0194	0.7765	−0.1897	0.0046†
FPG	0.1358	0.0445*	−0.0404	0.5465
TNF-α	0.0682	0.3186	−0.0356	0.5989
Adiponectin	−0.1771	0.0111*	0.1572	0.0227*
IL-6	0.3953	0.0000†	−0.0009	0.9890
IL-1β	−0.0804	0.2315	−0.0586	0.3781
CRP	—	—	0.0463	0.4849
PTX3	0.0475	0.4849	—	—

BW, body weight; CRP, C-reactive protein; DBP, diastolic blood pressure; FPG, fasting plasma glucose; HDL-C, high-density lipoprotein cholesterol; IL, interleukin; PTX3, pentraxin 3; SBP, systolic blood pressure; T-CHO, total cholesterol; TG, triglyceride; TNF-α, tumor necrosis factor-α; WC, waist circumference.
*$P < 0.05$; †$P < 0.01$.

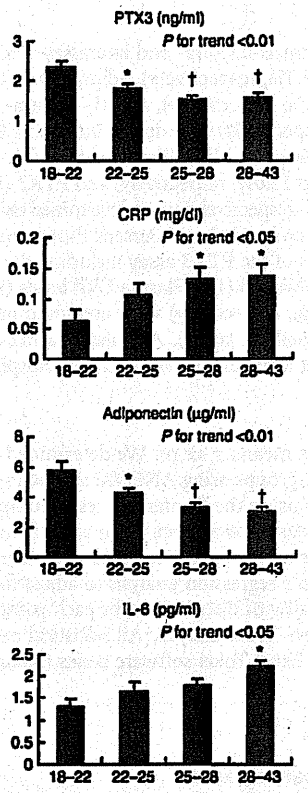

Figure 1 Plasma levels of pentraxin 3, C-reactive protein, adiponectin, and interleukin-6 in apparently healthy males. Participants were assigned to the following groups based on BMI as follows: group 1, 18–22; group 2, 22–25; group 3, 25–28; and group 4, 28–43. Data are shown as means ± s.e.m. *$P < 0.05$ and †$P < 0.01$ vs. 18–22 group. Plasma CRP ($P < 0.05$) and IL-6 ($P < 0.05$) levels significantly increased with increasing BMI, whereas plasma PTX3 ($P < 0.01$) and adiponectin ($P < 0.01$) levels significantly decreased with increasing BMI. Although plasma PTX3 levels in groups 2, 3, and 4 did not significantly differ, all of them were significantly lower than those in group 1. The findings for adiponectin were similar to those of PTX3. Plasma CRP levels in groups 3 and 4 did not significantly differ, but both were significantly higher than those in group 1. Plasma IL-6 was significantly higher in group 4 than in group 1. PTX3, pentraxin 3; CRP, C-reactive protein; IL-6, interleukin-6.

between PTX3 and CRP in obesity are in accordance with these reports.

Expression of the *PTX3* gene is stimulated by HDL-C in cultured human umbilical vein and aortic endothelial cells (16). Thus, the decrease in plasma HDL-C might be responsible for the lower PTX3 levels in obese individuals or in those with MetS. However, the cause of the decreased PTX3 level in obesity or MetS cannot be explained simply by a relationship between PTX3 and HDL-C, because we could not identify a positive association between them. We found that the PTX3 level positively correlated with adiponectin, an adipocyte-specific plasma protein with antiatherosclerotic properties. Systemic clinical hypoadiponectinemia is closely associated with obesity, type 2 diabetes and coronary artery disease. The increased oxidative stress in adipose tissue that accumulates in obesity results in decreased adiponectin production (17). A similar oxidative stress-related mechanism might also, at least in part, affect PTX3 production in adipocytes of obese individuals.

Whether plasma PTX3 increases to protect against local inflammation or to exacerbate the expansion of tissue damage remains unknown. However, mice with induced *PTX3* genes are more resistant to endotoxic shock induced by lipopolysaccharide and to polymicrobial sepsis caused by cecal ligation and puncture (18). Additionally, PTX3-deficient mouse models of acute myocardial infarction caused by coronary artery ligation developed more myocardial damage, and this phenotype was reversed by exogenous PTX3 (19). Taken together, current evidence indicates that PTX3 plays tissue protective and anti-inflammatory roles. Both PTX3 and CRP can bind C1q, the recognition subunit of the classical complement pathway, which might be activated by CRP after binding to C1q and such binding might also contribute to tissue damage. Although PTX3 enhances binding between apoptotic cells and C1q, it inhibits CH50 and C1q hemolytic activity when incubated with normal human serum or human C1q, suggesting that PTX3 inhibits the classical complement pathway (20). These findings indicate that decreased plasma PTX3 levels in obese individuals or those with MetS accelerate chronic inflammation and atherosclerosis. In addition, complement fraction C1q is structurally homologous with adiponectin and interaction with PTX3 and adiponectin should be considered. However, this notion also requires further investigation.